Structural Engineering Report No. 141

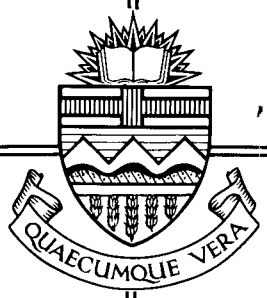

SHEAR-MOMENT TRANSFER IN SLAB-COLUMN CONNECTIONS

by
SCOTT D. B. ALEXANDER
SIDNEY H. SIMMONDS

JULY 1986

Structural Engineering Report No. 141

Shear-Moment Transfer in Slab-Column Connections

by

Scott D.B. Alexander

and

Sidney H. Simmonds

Department of Civil Engineering

University of Alberta

Edmonton, Alberta

July 1986

Abstract

This report describes a method for the analysis of slab-column connections at ultimate load which uses a truss analogy to model the flow of forces between the slab and column. Although general in application it is developed in detail for the case of a flat plate to edge column connection under combined shear and moment. The slab is unreinforced for shear and moment is about an axis parallel to the free edge.

A new mechanism to explain the punching phenomenon is proposed. This mechanism describes punching as the failure of the slab to confine concrete compression forces out of the plane of the slab.

The model is calibrated with results of 48 interior slab-column connection tests under shear load only. It is then used to analyze 43 edge connections from 8 separate investigations yielding excellent agreement between test and predicted results.

It is concluded that the capacity of a slab-column structure is defined by the lesser of two essentially independent capacities. These are the local slab-column connection strength and the overall slab strength as determined by yield-line or similar analysis.

Acknowledgements

This report is based on the M.Sc. thesis of the same title by Mr. S.D.B. Alexander undertaken under the supervision of Dr. S.H. Simmonds.

Financial assistance received from the National Science and Engineering Research Council for this study under Operating Grant A1691 is greatly appreciated.

Table of Contents

List of Tables

List of Figures

Notations

A_{bar}	area of single reinforcing bar
A_f	area of steel contributing to flexural portion of unbalanced moment
A_{sv}	flexural steel which is close enough to column in order to participate in shear strut
c	dimension of column face
c_1	column dimension perpendicular to the free edge
c_2	column dimension parallel to the free edge
d_{bar}	nominal diameter of reinforcing bar
d_s	effective depth of reinforcing mat measured from centre of mat to far side of slab
d'	cover of reinforcing mat measured from centre of mat to near side of slab
e_1	distance between bar parallel to free edge passing through column and front face of column
e_2	distance between flexural bar and nearest parallel column face
f_{cu}	cube strength of concrete
f'_c	cylinder strength of concrete
f_y	steel yield stress
f_u	steel yield stress
j	ratio of flexural moment arm to d_s
K	non-dimensional parameter used to estimate $\tan\alpha$
M_f	unbalanced flexural moment
M_v	unbalanced moment due to shear force distribution

s	reinforcing bar spacing
s_{eff}	effective tributary width of reinforcing bar
t	thickness of slab at slab-column connection
V_u	ultimate shear capacity
α	angle of concrete compression strut relative to horizontal
ρ_{sv}	ratio of A_{sv} to product of perimeter of slab-column connection and d_s
ΔF	unit bar force
ΔM	change in moment due to the reassignment of a unit bar force
ΔV	change in shear due to the reassignment of a unit bar force
T,B	superscripts denoting top mat and bottom mat respectively
1,2	superscripts denoting perpendicular and parallel to the free edge respectively

Chapter 1

Introduction

1.1 Description of Problem

The reinforced concrete flat plate is an economical and popular structural system. It consists of a two-way slab of uniform thickness cast monolithically with columns. Beams, drop panels and capitals are not used.

The flat plate has a number of advantages over other forms of reinforced concrete slab construction.

1. Simplified formwork speeds up construction and allows the flying of forms, thus reducing labour costs.
2. In high-rise residential buildings, the underside of the slab may be finished so as to provide an acceptable ceiling for the floor below.
3. In commercial buildings, mechanical and electrical services are not obstructed by beams, drop panels or capitals.

One of the major problems with flat plates is their susceptibility to 'punching' failures. These are local failures of the slab-column connection in which the column together with a portion of the slab push through the slab. The unpredictable nature of this type of failure is a major drawback to flat plate construction.

Much of the work to date has dealt with interior columns under vertical load only (no net moment tranferred between the slab and column). With moment tranferred between

the slab and the column, however, the vertical load capacity of the connection is reduced. The combination of shear and unbalanced moment is unavoidable at edge and corner column locations. It occurs at interior columns as well, as a result of unequal spans, patterned loading or lateral loading.

While some reasonably accurate procedures have been developed for the prediction of punching strengths under balanced loading, efforts to extend them to cases of combined shear and moment have met with limited success. Design procedures tend to be extremely conservative with the result that designers may opt for beams, drop panels, capitals or some form of shear reinforcement, thereby forgoing many of the advantages of the flat plate. A reliable method for predicting the ultimate behavior of a slab-column connection, without shear reinforcement, under any combination of shear and moment would permit the increased use of this economical structural system.

1.2 Scope

This thesis develops the components of a general analytical model for the prediction of local or punching failures of slab-column connections. The approach uses a truss analogy to describe flow of forces within the connection at ultimate load.

A comparison is made between model predictions and the results of forty-three edge column tests. Edge column tests

were chosen beacause they provided a wide range in test apparatus, specimen scale and moment-shear combinations.

All edge column tests used here conform to the following criteria:

1. the unbalanced moments were about an axis parallel to the free edge of the slab.
2. slabs contained no shear reinforcement or beams.
3. slabs had no large perforations near columns.
4. normal weight concretes were used throughout.

None of these criteria is a result of some inherent limitation of the analytical model. The model is capable of handling moments about any axis as well as interior and corner slab-column connections. Slabs with beams, shear reinforcement and perforations are not treated although it will be seen that these cases do not present any conceptual hurdles.

Chapter 2

Background

A general analytical model for a slab-column connection should predict both the ultimate capacity of the connection and the mechanisms by which load is carried. This chapter outlines the reasons for using a truss analogy.

Information regarding the behavior of slab-column connections near failure is reviewed. Some of the elements of existing analytical models are assessed in terms of how well they conform to observed behavior. From this it is concluded that the truss analogy is the most promising approach for modelling a slab-column connection.

2.1 Description of Failure

The term 'punching' is often used to describe the failure of a slab-column connection. It is associated with a particular collapse mechanism in which the column together with an attached portion of slab push through the slab. The slab breaks along a sloping surface which extends from the compression side of the slab at the face of column to the tension side of the slab at some distance from the column. The average angle of the failure surface relative to horizontal is usually between 25° and 30°.

For cases of balanced load (no net moment transfer between the slab and the column), the inclined surface surrounds the column. The result is the classic punching failure surface in the shape of a truncated cone or pyramid.

Cases of unbalanced load have a combined failure mode although they are still often described as punching. The punched region is confined to the area near the more heavily loaded face of the column. The two adjacent side regions show extensive torsional cracking while the area near the opposite face may show little or no distress. Figure 2.1 illustrates three typical punching failures as seen from above. Note that there is a striking similarity between the failure of the edge column and the that of the interior column under combined shear and unbalanced moment.

Punching failures follow a fairly predictable sequence of events. Masterson and Long[9] described four basic stages in the punching failure of an interior column.

1. Flexural and shear cracks form in the tension zone of the slab near the face of column.
2. Slab tension steel close to the column yields.
3. Flexural and shear cracks extend into what was the compression zone of the concrete.
4. Failure occurs before yielding extends beyond vicinity of column. Masterson and Long assumed punching was caused by a rupture of the reduced compression zone in the slab.

The state-of-the-art report by Regan[12] adds further details to this description. Near ultimate load, strain gradients in the slab near the column are extremely steep. Concrete strains are further concentrated at column corners. Steel strains are highest in bars which pass through the

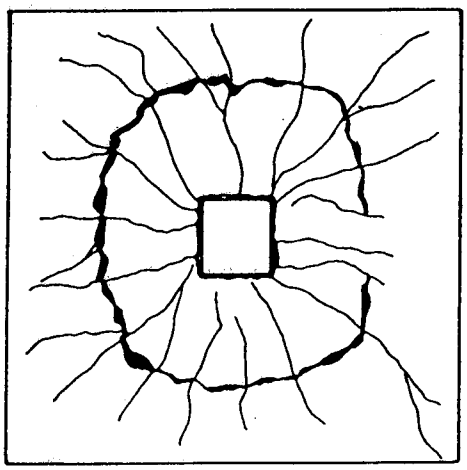

Shear Only

(after Van Dusen)

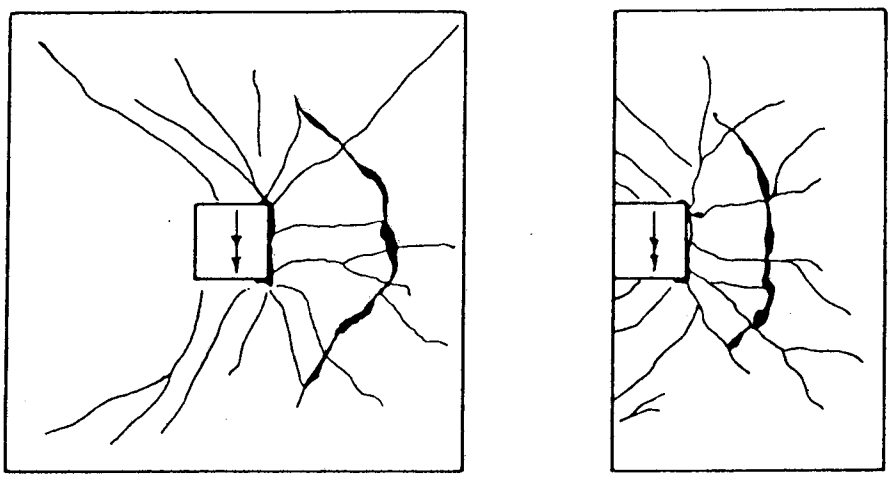

Moment and Shear

Figure 2.1 Typical Punching Failures

column although there may be strains sufficient for yielding in bars which do not. Efforts to predict punching failure on the basis of some limiting strain criteria so far have not been successful.

From the shape of the failure surface, it might appear that diagonal cracking of the concrete plays an important role in punching failures. However, test results indicate that such cracking forms at loads in the order of 50% to 70% of ultimate. Furthermore, a slab-column connection in this cracked state is very stable since it may be unloaded and reloaded without affecting ultimate capacity.

2.2 Requirements of General Analytical Model

Hawkins[4] grouped existing analytical models for shear and moment transfer in slab-column connections into three categories.

1. Models based on a linear distribution of shear stress on some critical section. This is perhaps the simplest approach and is favoured by most design codes.
2. Models based on beam analogies. Beam analogies describe a slab-column connection as the junction of orthogonal beam elements contained within the slab. The net shear-moment capacity of the connection is assumed equal to the sum of the shear, torsional and flexural capacities of these beam elements. Several beam analogies have been proposed and their differences lie largely in the method by which shear and torsional

strengths are calculated and in the degree of redistribution allowed between beam elements.

3. Models based on plate theory. In addition to simple elastic plate models, this classification includes more sophisticated approaches which can account for cracking and plastic behavior such as finite element analyses. All of these models assume that the reinforcement can be adequately described as a thin membrane rather than discrete bars.

In a detailed discussion of these models, Van Dusen[20] outlined several of their weaknesses. His discussion, together with the known characteristics of a punching failure, provides some guidance for the development of a general analytical model.

2.2.1 Shear Strength

All linear stress distribution models and most beam analogies assume vertical load is carried by shear stress on some critical section. The critical section is a vertically oriented surface at some distance from the face of column. A nominal shear stress based upon the applied loads and the geometry of this section is calculated.

The description of a punching failure suggests that it is unlikely that vertical load on a slab-column connection is controlled by shear stress on some vertical plane. This stress state requires a diagonal tension field in the concrete. However, diagonal cracking at a relatively early

load stage should preclude the tension field. At the very least, the area of concrete available to participate in this mechanism ought to be confined to the uncracked region in the compression zone of the slab at the face of the column. In spite of this, most critical sections are placed at some distance from the column and the area of the critical section is based on the depth of the reinforcement rather than the thickness of the compression zone.

A more plausible source of shear strength is an inclined compression field in the concrete. Together with steel tension ties, this approach is often referred to as a truss model. Truss models are currently recognized by CAN3-A23.3 in its general provisions for shear and torsion in beams. Not only does this mechanism provide a load path for shear forces in the presence of diagonal cracking, it explains the role that flexural reinforcement plays in determining shear strength.

2.2.2 Reinforcement

While it is generally agreed that flexural reinforcement has an effect on the shear strength of a slab-column connection, some analytical procedures neglect it completely. Those which do not, usually assume a smooth distribution of slab reinforcement. This idealization has three main drawbacks. First, slab reinforcement is discrete. At collapse, a bar either crosses a failure surface or it does not. An average density of reinforcement does not

account for this. Secondly, reinforcement is often irregularly spaced making smooth distributions difficult to define. Finally, given design moments and shears based on smoothly distributed reinforcement, there is no clear indication as to where a particular bar is best placed.

It would be desirable to treat slab reinforcement as a series of discrete bars rather than an average density. By considering reinforcing bars individually, an analysis would not be limited to any particular reinforcing pattern. The designer would be given a clear idea as to how the placement of reinforcement affects the behavior of the connection. Furthermore, large variations in steel strains, even among bars passing through the column, could be accounted for.

2.2.3 Critical Section

Except for analytical solutions such as finite element, most methods of analysis require the definition of some critical section. For linear stress distribution models, this is the surface upon which nominal shear stresses are based. For beam analogies, the critical section defines the geometry of the beams which frame into the connection. In either case, there are fundamental problems associated with the assumption of any particular critical section.

The shape of the failure surface changes with the ratio of moment to shear. This being the case, it is hard to imagine why a critical section which attempts to describe the punching phenomenon should also be relevant to a

torsional failure in the side regions of a slab-column connection under unbalanced moment. Van Dusen suggested that this problem might be remedied by making the critical section a variable of the model. To some extent, this is the approach taken by Zaghlool[21].

There also arises the question of what to do with slab discontinuities, such as reinforcing bars, which are located at or very near the assumed section. In the case of reinforcement, a popular solution is to use distributed reinforcing ratios rather than discrete bars. This, however, amounts to covering up one inaccuracy with another. Perhaps a better solution is to determine an effectiveness of reinforcement based upon its proximity to the column.

2.2.4 Variables

At minimum, a slab-column connection which is unreinforced for shear can be defined by the following variables.

1. The overall geometry of the connection.
2. The concrete strength.
3. The strength of the flexural reinforcement.
4. The placement of the flexural reinforcement.

Any analytical model which is expected to predict both ultimate capacity and behavior must account for variations in any of these parameters.

As output, the analytical model should provide a complete range of load combinations which will cause

collapse. A failure envelope for all possible ratios of moment to to shear is required. In addition to this, the magnitude of in-plane forces may have to be accounted for.

2.3 Truss Model Approach

One of the conclusions reached by Van Dusen was that the behavior of a slab-column connection might be predicted with a truss model. He proposed the truss model for an edge column illustrated in Figure 2.2. This is believed to be the only reference in the literature which uses a truss model to describe the flow of forces in a slab-column connection.

Van Dusen did not develop the model beyond a conceptual stage and his assessment of it was strictly qualitative. He noted that the configuration of concrete compression struts is in good agreement with observed crack patterns. Shear is carried by the vertical components of the inclined concrete struts, a mechanism which is not hampered by the formation of diagonal cracking. Moment is developed by conventional flexure but the amount of flexural steel which can be developed is partly dependent on the amount of transverse reinforcement.

Van Dusen foresaw two major difficulties in developing the truss model. The first of these was in estimating the actual stress within each strut and the critical failure stress with which to compare it. His other concern was in establishing limits for the inclination of the compression struts. In addition to these problems, it should be noted

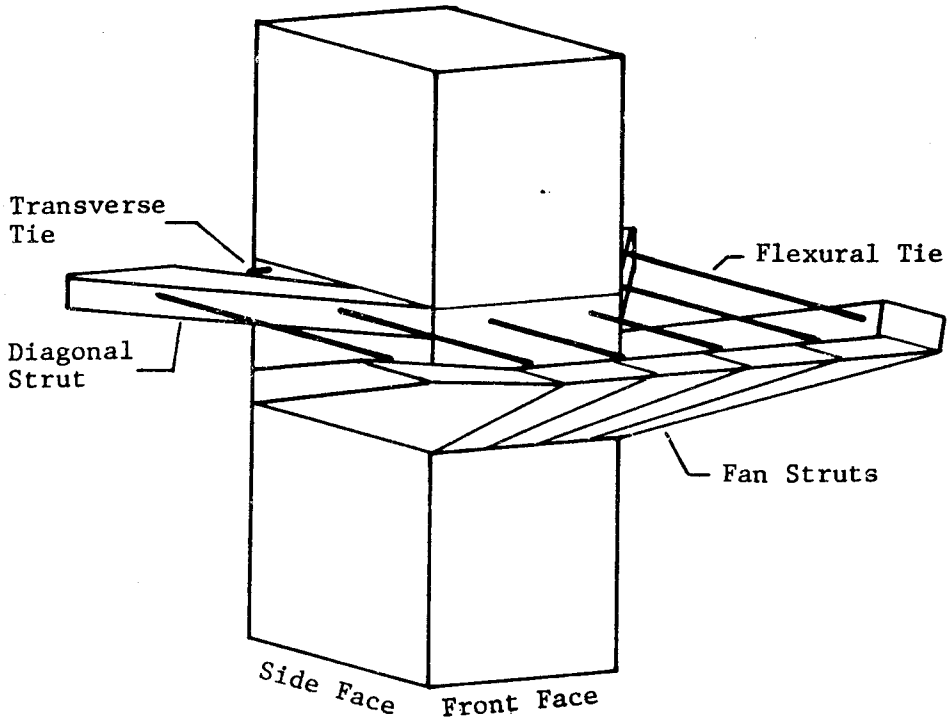

(after Van Dusen)

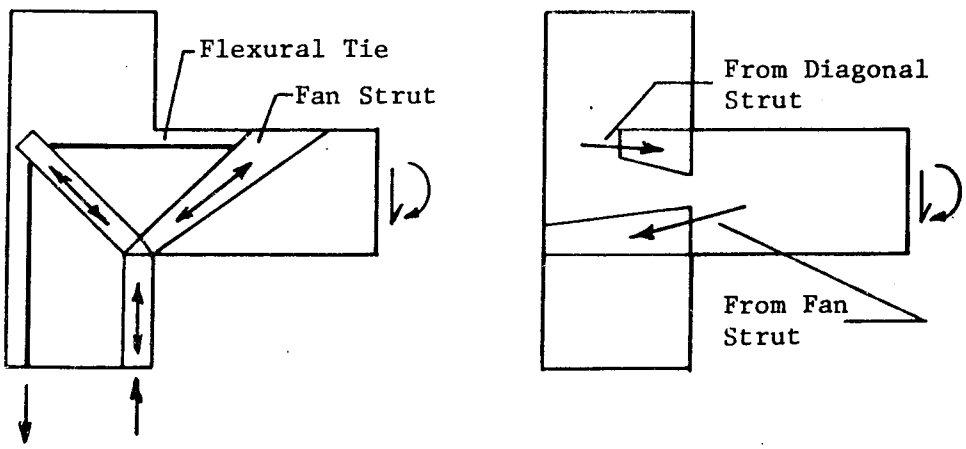

(a) Section Through Front Face

(b) Forces on Side Face

Figure 2.2 Van Dusen's Truss Model for an Edge Column

that the truss configuration proposed by Van Dusen can model only a narrow range of moment to shear ratios. Some means of extending the model to handle a complete range of shear-moment combinations is required. Finally, existing truss models for beams rely on shear reinforcement to provide necessary transverse tensile forces. A truss model for a slab-column connection which has no shear reinforcement requires some different mechanism to handle the tensile forces which are out of the plane of the slab.

In spite of its lack of quantitative support, the truss model is considered to be the most promising approach to the problem of shear and moment transfer in slab-column connections. It describes the flow of forces within a connection in a way which is consistent with observed cracking and it provides a physical mechanism by which flexural reinforcement participates in providing shear capacity. In subsequent sections, the truss model is developed into a usable analytical tool for slab-column connections which are not reinforced for shear.

Chapter 3

Elements of the Truss Model

Truss models can be used to describe the behavior of any slab-column connection at ultimate load. In Chapter 4, the particular case of the edge column will be considered. The basic components and mechanisms described in this chapter are general and may also be used to construct interaction diagrams for interior and corner columns.

3.1 Model Components

The model consists of a three dimensional space truss composed of concrete compression struts and steel tension ties. The arrangement of reinforcing steel and fan-like compression fields proposed by Van Dusen is broken down into individual bar-strut units.

There are two types of compression struts:

1. those parallel to the plane of the slab (in-plane or anchoring struts) and
2. those at some angle (α) to the plane of the slab (out-of-plane or shear struts).

3.1.1 In-Plane or Anchoring Struts

Four anchoring struts are shown in Figure 3.1. Each is equilibrated by two mutually perpendicular reinforcing bars. One bar passes through the column, parallel to the axis about which the unbalanced moment is acting and the other is some distance from the column. The bars and struts lie in a

plane parallel to the plane of the slab. Through this mechanism, bars at some distance from the column are able to exert moment on the connection by flexure.

The compression strut meets the column face at the front corner of the column. Equilibrium of the entire bar-strut assembly is satisfied by summing moments of the bar forces about this point.

3.1.2 Out-of-Plane or Shear Struts

As a starting point, consider the force diagram for a corbel illustrated in Figure 3.2(a). Three quantities are significant in determining the geometry of this force triangle. They are the strut angle (α), the magnitude of the tensile force in the steel tie and the magnitude of the compressive force in the concrete strut. Satisfaction of equilibrium constrains any one of these quantities to be a function of the other two. Furthermore, α is predetermined because the loading point coincides with the conjunction of the tensile and compressive forces. If a local failure in reinforcement anchorage does not govern, then the ultimate capacity of the corbel is defined by either the failure of the compression strut or the tension tie, whichever comes first.

The ultimate capacity of a shear bar-strut unit in a slab-column connection (shown in Figure 3.2(b)) is in part determined by the same variables which govern a corbel. There are, however, added complications not present in a

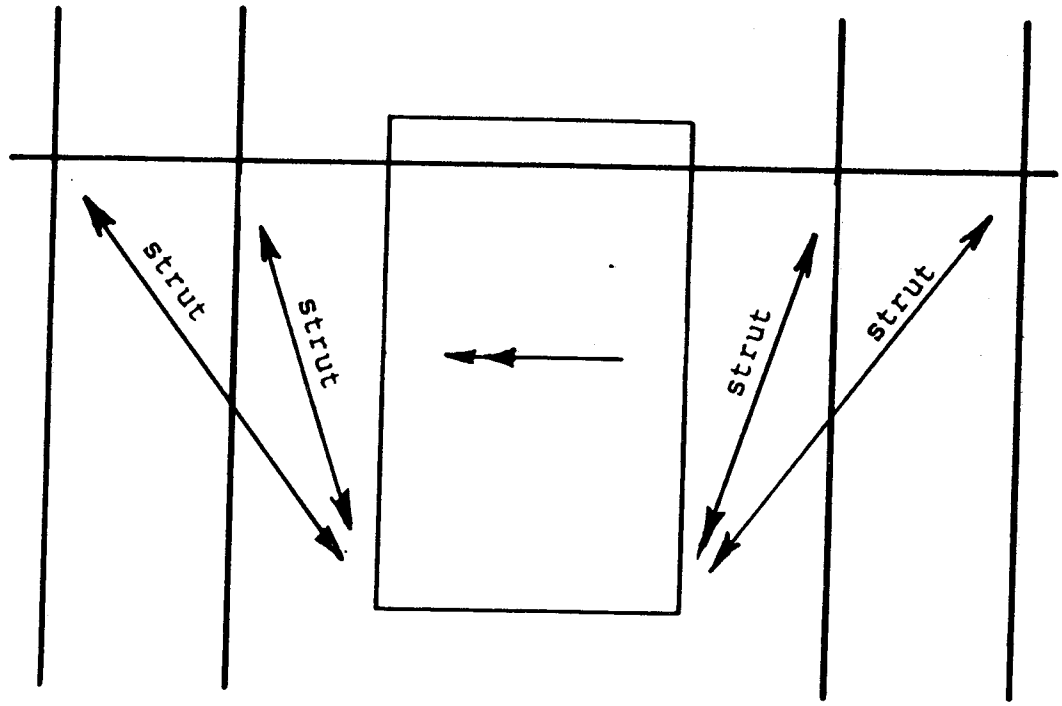

Figure 3.1 In-Plane or Anchoring Struts

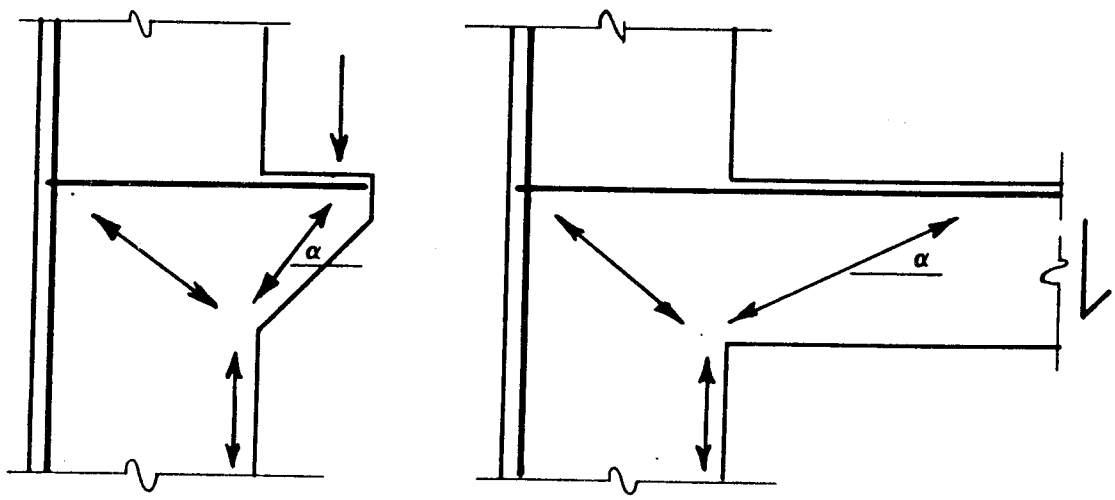

Figure 3.2 Comparison of Corbel with Out-of-Plane or Shear Strut

typical corbel. In general, the point of load application in a slab will not coincide with the junction of the tensile and compressive force. As a result, α is not preset by the position of the load. Even more important is the fact that the shear or vertical component of the compression strut is no longer equilibrated at the bar-strut junction by the applied load. There exists a force component out of the plane of the slab which must be balanced by some form of tension field within the concrete.

3.1.3 Shear Steel

For a corbel, the amount of steel participating in the tension tie is clearly defined. This is not the case for a slab-column connection. Therefore, a certain amount of steel must be assumed capable of developing a compression strut into the column by virtue of its proximity to the column. This steel is designated as shear steel (A_{sv}). Superscripts of 'T' and 'B' will refer to top and bottom mat respectively.

It seems reasonable to assume that the shear steel includes all steel passing through the column. In addition, it is felt that steel within d_s of the column is at least partly effective in developing a compression strut, depending upon its distance from the column face. Therefore, A_{sv} is assumed equal to the sum of all steel passing over the column periphery plus a fraction of that steel within d_s of the column face. This fraction decreases linearly from

unity for a bar at the column face to zero for a bar located d_s from the column face.

3.2 Ultimate Conditions

Criteria are required to establish the ultimate capacity of a bar-strut combination. Two failure modes have been identified, namely the failure of the tension tie or the compression strut. In the particular case of a shear strut however, the presence of an out-of-plane force at the bar-strut junction which is not equilibrated by the external load at that point creates an additional possibility. There may be a failure in which the out-of-plane component of the compression strut exceeds the confining strength of the slab.

3.2.1 Primary Assumption

It is assumed that the shear steel will always reach yield. Therefore, a compression failure of the concrete strut will never govern. This is a significant departure from conventional truss models in which the determination of compression strut geometry and the resulting concrete stresses is considered of major importance. Furthermore, it is almost certainly false if the connection is reinforced heavily enough.

Two points, however, justify the assumption:

1. Most of the existing test data show that steel in the immediate vicinity of the column yields prior to

failure. This suggests that the conditions which lead to the compression strut capacity defining ultimate capacity are not typical of slab-column connections.

2. Predicting compression failure of concrete would rely on an extensive set of assumptions, both to estimate the axial stresses within the struts and to define some critical concrete stress with which to compare them. The dubious accuracy of this procedure coupled with the observation that compression failure of concrete is not ductile make this a failure mode to be precluded rather than described. It is likely that limitations on the density of reinforcement in a slab-column connection will be required to ensure that the compression struts do not govern.

3.2.2 Strut Capacities

As a consequence of the above assumption, the ultimate capacity of an in-plane bar-strut unit is limited only by the yield of the participating reinforcing bars. No attempt is made to check the stresses within the concrete compression strut.

In the case of a shear bar-strut unit, the bar force alone is not sufficient to define the ultimate capacity. The angle of the compression strut is vital to determining its contribution to shear. The ultimate capacity is reached with the bar at yield and α at some critical value.

3.3 Calibration of α

To complete the description of a shear strut, some means of estimating α is required. A non-dimensional, empirical approach similar to that commonly used in hydraulic engineering is taken. Those parameters which are felt likely to affect α are assembled in a non-dimensional term. This term is then related through experimental results to α.

3.3.1 Factors Affecting α

Section 3.2 presented a new explanation for shear failure in which the slab is unable to contain the out-of-plane component of a shear strut. From geometric considerations, $\tan\alpha$ is equal to the ratio of the out-of-plane component to the in-plane component of the compression strut. Since A_{sv} is always assumed to reach yield, the in-plane component of a compression strut is equal to the yield force of its attendant tie back steel. The maximum out-of-plane component is some function of the ability of the slab to confine the bar. Three parameters can be used to describe this confining strength:

1. the tributary width of each reinforcing bar (s),
2. the cover of the reinforcement (d') and
3. the strength of the concrete.

The particular concrete strength in question is most likely the tensile strength. However, the tensile strength of concrete is not consistently reported by investigators nor

is it generally recognized by building codes as a basis for design. Therefore, it will be assumed proportional to $\sqrt{f'_c}$ (with appropriate units of stress).

3.3.2 Interior Column Tests

Since only shear struts are affected by α, the ideal test set-up for estimating it would be one where only shear struts are present. Bar spacings in the region of the column should be reasonably constant. Furthermore, the point or points of load application on the slab should be remote from the column in order to separate the confining strength of the slab from the confining effect of the load.

The literature contains many test results on interior columns which fulfill these requirements. These tests consist of slabs supported on the perimeter with axially loaded columns in the middle.

In order to apply the model to any slab-column connection, a method of assessing conditions on a particular column face is required. By treating each face independently, the effects of column rectangularity and asymmetry of reinforcement, geometry or loading will be accounted for automatically. For the purposes of calibration, however, there must not be differences between the four column faces of each test. Therefore, only square column tests are used.

3.3.3 Procedure

For each test, the experimental measure of tanα is taken as the ratio of the failure load to the total area of top mat shear steel (A_{sv}^{T}) times its yield strength. This is plotted against a non-dimensional factor K.

Originally, K was taken as the ratio of the product of s, d_s and $\sqrt{f'_c}$ to the yield force of one bar. However, some geometric effects were anticipated. Hawkins *et al*[5] reported reduced apparent shear strengths with increased column rectangularity. To preserve the independence of each column face, this effect was accounted for by adding the dimensionless factor of c/d_s, where c is the column dimension perpendicular to the bar being considered and d_s is the effective depth of the slab. Finally, a maximum ratio of s to d' was found beyond which increases in s did not increase tanα. For regular bar spacings, this ratio is approximately equal to six. Therefore, the effective tributary width on either side of a reinforcing bar is one half of the centreline spacing to the next bar in the same mat, to a maximum of 3d'. In the expression for K, s is replaced with s_{eff}. The resulting definition for K is:

$$K = \frac{s_{eff} \times d' \times \sqrt{f'_c}}{A_{bar} \times f_y \times (c/d_s)^{0.25}}$$

The power of 0.25 for was arrived at by trial and error.

Figure 3.3 shows a plot of tanα against K. It suggests a function which passes through the origin and

asymptotically approaches a value of unity. The function was assumed to be of the form:

$$\tan\alpha = 1.0 - e^{-aK^n}$$

Performing a regression of the interior column data (in Imperial units) against this form of function produced the following results.

$$a = 0.95 \quad \text{and}$$
$$n = 1.09$$

The regression equation is shown in Figure 3.4. To provide a more convenient design equation, the value of n was set to unity, resulting in the following equation (shown in Figure 3.4).

$$\tan\alpha = 1.0 - e^{-2.25\,K} \qquad \text{(SI)}$$

or

$$\tan\alpha = 1.0 - e^{-0.85\,K} \qquad \text{(Imperial)}$$

where stresses are in MPa for SI units and ksi for Imperial units. The design curve closely follows the regression curve for lower values of K and is slightly conservative for higher values.

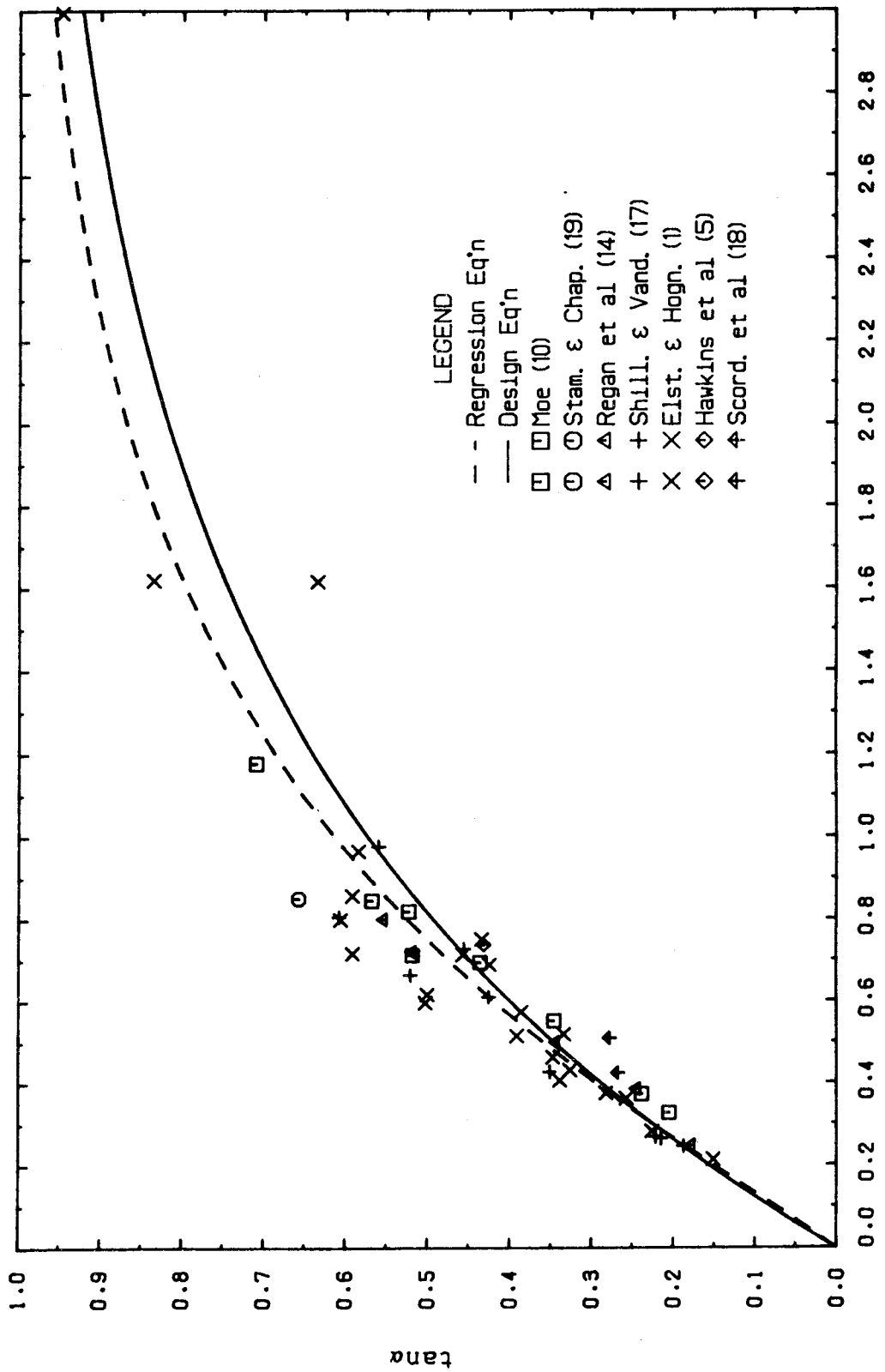

Figure 3.3 Calibration of α

3.4 Summary

All of the elements required to assemble a truss model for any slab-column connection have been defined. Briefly, these elements are:

1. an in-plane or anchoring strut which provides a mechanism for increasing the flexural moment transferred to the column at the expense of shear capacity on the side faces.
2. an out-of-plane or shear strut which accounts for shear and, on the front column face, flexure.
3. a method of estimating α, required to set the geometry of each shear strut.

In Chapter 4 these components are used to develop the shear-moment interaction for the particular case of the edge column.

Chapter 4

Shear-Moment Interaction at an Edge Column

The model components outlined in the preceding chapter are of general application. In this chapter, they are used to develop an interaction diagram for the particular case of an edge column.

For convenience, the following designations are applied to the various bars contributing to A_{sv}. Superscripts of 'T' and 'B' still refer to top and bottom mat steel respectively. Additional superscripts of '1' and '2' refer to bars perpendicular and parallel to the free edge.

4.1 Preliminary Considerations

Figure 4.1 shows a shear-moment interaction curve for an edge slab-column connection. It is similar to a column interaction diagram. Four basic control points (A, B, C and D) are defined on the interaction diagram. Each has an inverse counterpart (A', B', C' and D') in which the directions of the net shear and moment vectors are reversed. For clarity, a distinction will be made between shear struts which oppose the downward movement of the slab relative to the column (gravity shear struts) and shear struts which oppose the upward movement of the slab relative to the column (uplift shear struts).

The control points A, B, A' and B' mark the boundaries of two distinct types of interaction behavior. Between A and B and between A' and B' are regions of shear-moment

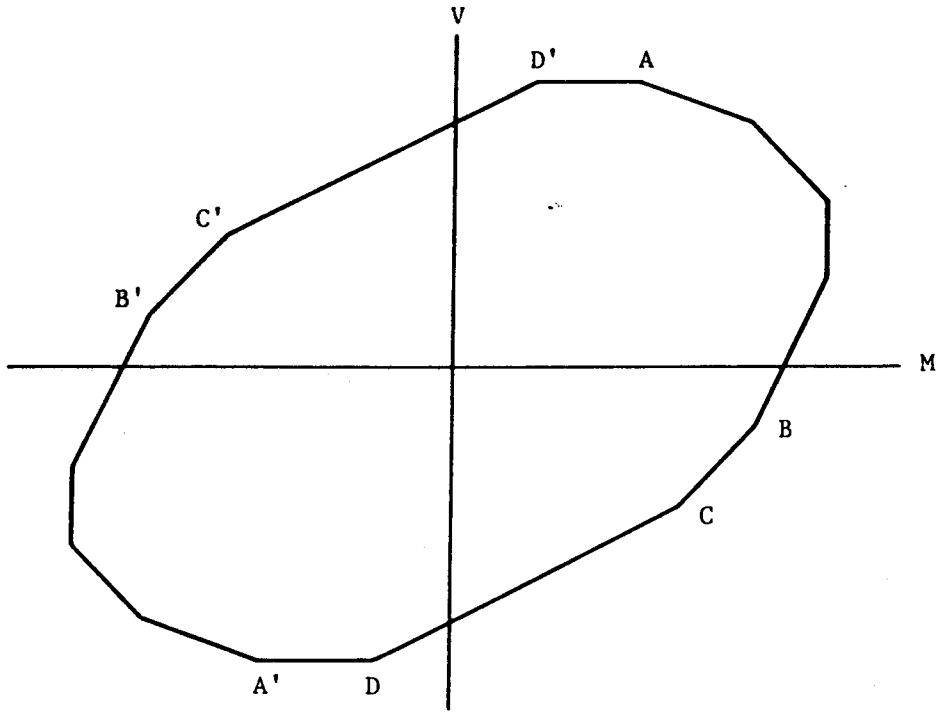

Figure 4.1 Typical Interaction for Edge Column

interaction on the side faces. The utilization of the shear steel perpendicular to the free edge remains constant. Between B and A' and between B' and A, there is a reversal of the orientation of the shear struts tied by the shear steel perpendicular to the free edge. This could be described as a shear-flexure interaction on the front face. Control points C, D, C' and D' describe the intermediate stages of the shear-flexure interaction.

Three quantities are calculated for any point on the interaction diagram. They are the ultimate shear (V_u), the shear moment (M_v) and the flexural moment (M_f).

4.1.1 Sign Convention

For the purposes of constructing an interaction diagram, the following sign convention will be used for shear and moment:

1. a shear resulting from downward loading of the slab and an upward reaction by the column is positive.
2. an unbalanced moment which causes tension at the top surface and compression at the bottom surface of the slab is positive.

This sign convention is consistent with those of other shear-moment interaction diagrams presented in the literature. The practical range of shear-moment combinations is in the upper right quadrant of the diagram.

4.1.2 Ultimate Shear (V_u)

V_u is the net out-of-plane component of the concrete compression struts. The horizontal component of each strut is defined by the yield force of its attendant reinforcing bar. The vertical component is limited by the strut angle. To account for possible variations in yield stress, area of bar and strut angle, each shear bar-strut unit is treated individually. Therefore, V_u is the summation of these individual vertical components.

4.1.3 Shear Moment (M_v)

In order to estimate M_v, it is necessary to make some assumptions as to where each strut acts relative to the

column in plan. All compression struts act somewhere on the column perimeter. Any shear strut equilibrated by a reinforcing bar crossing the face of the column is assumed to be centred on that bar. Shear struts developed by steel between the column face and d_s from the column face are assumed to act at the front corners of the column.

Given the above distribution of shear struts around the column perimeter, it is possible to calculate the shear moment by summing moments of the vertical components of the struts about some axis parallel to the free edge of the slab. For the purposes of this investigation, moments are summed about the column centreline although the choice of axis is somewhat arbitrary. It matters only that the interaction diagram and the applied moments in the structure be calculated about the same axis.

4.1.4 Flexural Moment (M_f)

In general, any developed steel perpendicular to the free edge produces moment by direct flexure. In addition to shear steel, this developed steel includes bars perpendicular to the free edge which are tied to the column by virtue of in-plane struts. If this steel is denoted as A_f then M_f can be approximated by the expression:

$$M_f = A_f \times f_y \times jd_s$$

For ease in calculation, j is taken as a constant equal to

0.9. Note that the flexural contribution to the unbalanced moment is independent of both the position of the axis about which the shear moment is calculated and the value of α.

4.2 Control Points A and A'

At point A, all top mat shear steel is utilized in equilibrating gravity shear struts. Its counterpart, A', occurs when all bottom mat shear steel equilibrates uplift shear struts. Both A and A' are described schematically in Figure 4.2. These points are similar to a conventional corbel and set the limits for shear capacity of the connection.

Point A defines the maximum gravity shear capacity of the slab column connection.

$$V_u = \Sigma[A_{sv}^{T} \times f_y \times \tan(\alpha)]$$

Since only shear steel is developed to the column, A_f is equal to A_{sv}^{T1} giving:

$$M_f = A_{sv}^{T1} \times f_y \times 0.9 \times d_s$$

4.3 Control Points B and B'

Under unbalanced moment, the slab attempts to rotate relative to the column about an axis parallel to the free edge. The position of this axis varies with the ratio of

moment to shear. Control points B and B' describe a condition in which the axis is located in the slab at a distance from the free edge, slightly greater than column dimension (c_1). These two control points are illustrated in Figure 4.3.

At control point B, as at A, the steel which makes up A_{sv}^{T1} ties gravity struts. However, all of A_{sv}^{T2} between the free edge and the front face of the column is equilibrating in-plane struts. This provides the maximum anchorage for top steel perpendicular to the free edge to develop flexurally at the expense of all gravity shear strut capacity on the side faces. Any bottom shear steel parallel to the free edge resists the rotation of the slab relative to the column by developing uplift shear struts. This increases the shear contribution to unbalanced moment but there is a further reduction in the net shear capacity for the connection.

At point B', the axis of rotation is in the same position as it was at point B but the direction of rotation between the slab and column is reversed. As a result, on the side face, A_{sv}^{B2} is tied to in-plane struts while A_{sv}^{T2} steel equilibrates gravity struts. On the front face, uplift shear struts are tied by A_{sv}^{B1}.

4.4 Control Points C, C', D and D'

Throughout the interaction between points A and B, the orientation of the shear struts tied by A_{sv}^{T1} remain constant. However, between points B and A' and between points B' and

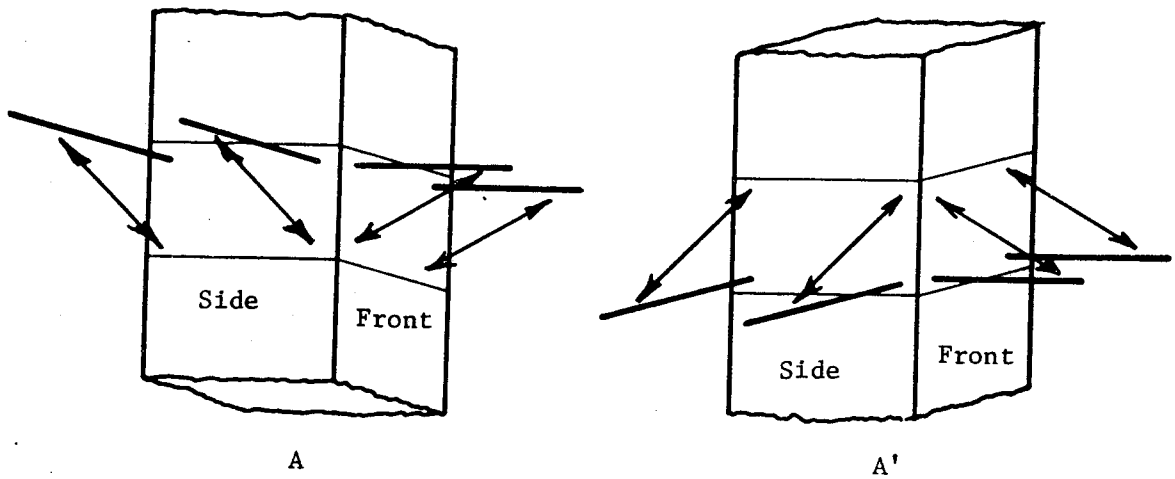

Figure 4.2 Control Points A and A'

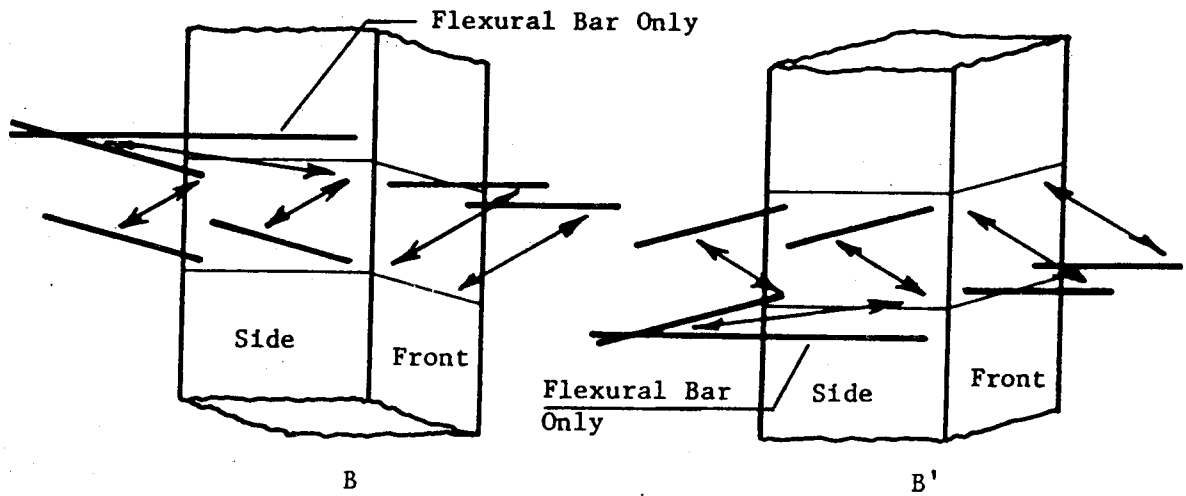

Figure 4.3 Control Points B and B'

A, the orientation of these shear struts on the front face of the column is reversed. A two-stage transition between between gravity and uplift shear struts on the front column face is proposed.

The flexural stage (control points C and C') is illustrated in Figure 4.4. At this stage, the shear struts on the front face have rotated so that they are parallel to the slab and contribute to flexure only. No shear struts are tied by steel perpendicular to the free edge. However, the flexural contribution of this steel is at the maximum defined by either point B or B'.

The inverted shear stage (control points D and D') is illustrated in Figure 4.5. This stage is analagous to a simply supported truss since, on the front face of the column, uplift shear struts are not tied by bottom bars and gravity shear struts are not tied by top bars.

The procedure already developed for estimating α cannot be applied to the inverted shear strut. Although the out-of-plane force component must still be confined by some form of tension field in the concrete, it is no longer clear what depth of concrete participates. Furthermore, the horizontal component of the strut is not necessarily related to the yield force of any bar.

A simple procedure is to assume that the ultimate capacity at control points D'and D can be approximated by using the capacities of the adjacent control points A and A' repectively. The ultimate shear capacity at point D' is

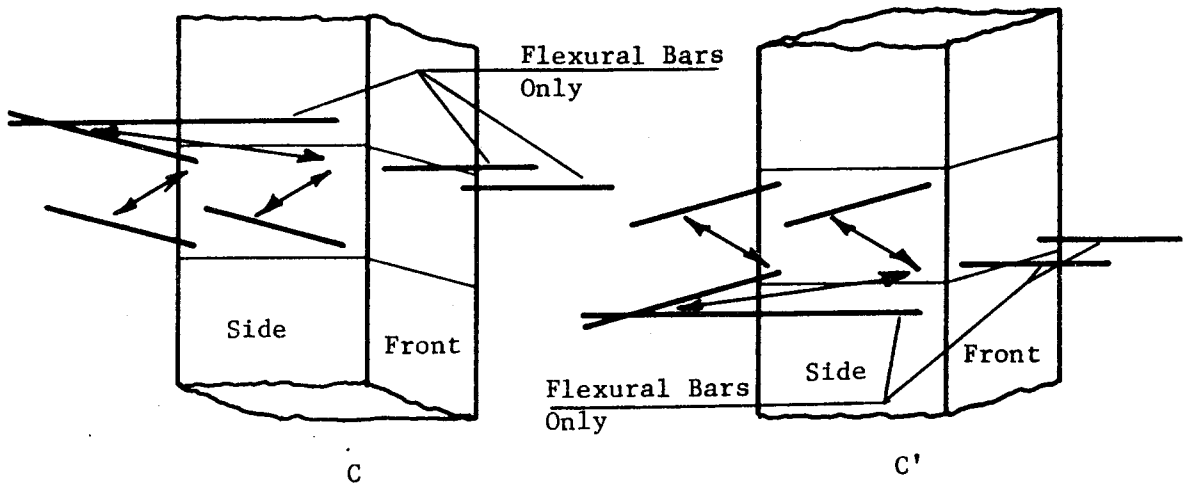

Figure 4.4 Control Points C and C'

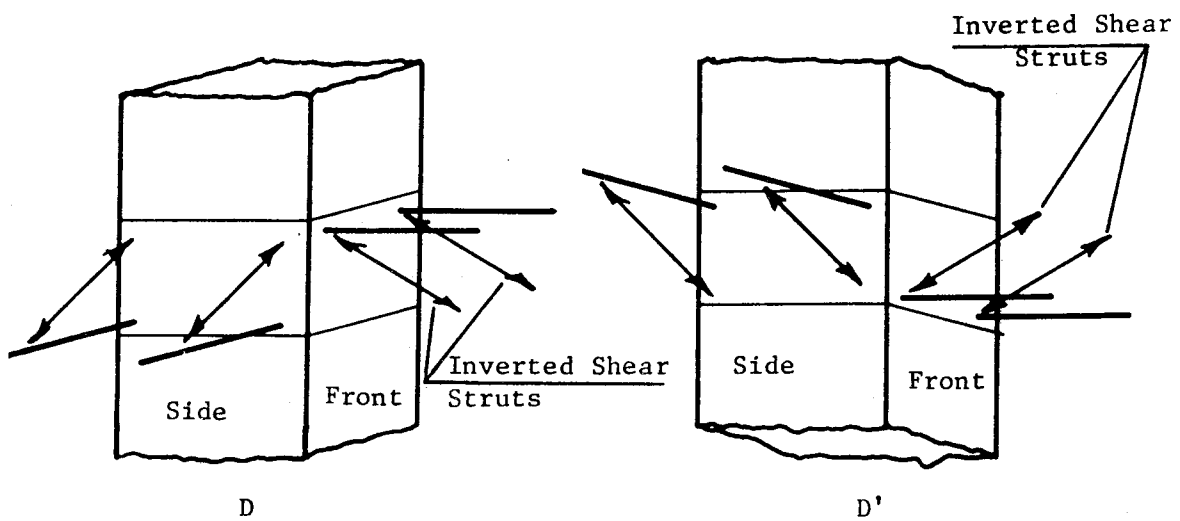

Figure 4.5 Control Points D and D'

assumed equal to that of point A. The ultimate moment at D' is assumed equal to the shear moment at A. Similarly, the capacity at control point D is defined in terms of A'. Therefore, in moving either from A to D' or from A' to D, only the flexural component of M_u is lost. It will be shown later that, although this procedure is not based on any physical mechanism, it usually gives conservative results.

4.5 Interaction Between Control Points

From point B through C and D to A' and from point B' through C' and D' to A, the interaction diagram is defined by straight line interpolation between the control points. All that remains is to develop the interaction from point A to B and from point A' to B'.

The slab-column connection may be viewed as having an overall symmetry about the plane of the slab. If the slab is reinforced with identical mats top and bottom, then the interaction diagram will be point symmetric. Since only the directions of moments and shears are reversed, a procedure developed for the interaction diagram between points A and B can also be used between points A' and B'. The development of this procedure for the region of interaction diagram between points A an B will be presented here.

The proposed transition between points A and B accounts for the effects of discrete reinforcement. A number of intermediate stages are defined and straight line interpolation is used between them.

A new stage is reached wherever the slope of the interaction diagram changes. This occurs when:

1. the in-plane struts complete the flexural development of a top bar perpendicular to the free edge or
2. a top bar parallel to the free edge is fully utilized by an in-plane strut or
3. a bottom bar parallel to the free edge is fully utilized by an uplift strut.

Note that part of the yield force of a particular bar can be used to equilibrate an out-of-plane strut while the balance equlilbrates an in-plane strut.

To proceed with the interaction diagram starting at control point A, the top bar which is closest and parallel to the free edge develops an in-plane strut first. Once it is fully devoted to an in-plane strut, then either the next closest top bar is developed in a similar fashion or the bottom bar closest and parallel to the free edge develops uplift. Since both the in-plane strut and the uplift strut enhance moment capacity at the expense of shear, some criterion is required to determine the order in which they develop.

It is felt that the interaction diagram must be convex. Therefore, the mechanism (in-plane or uplift) which develops first will be the one which is the most efficient at developing moment at the expense of shear.

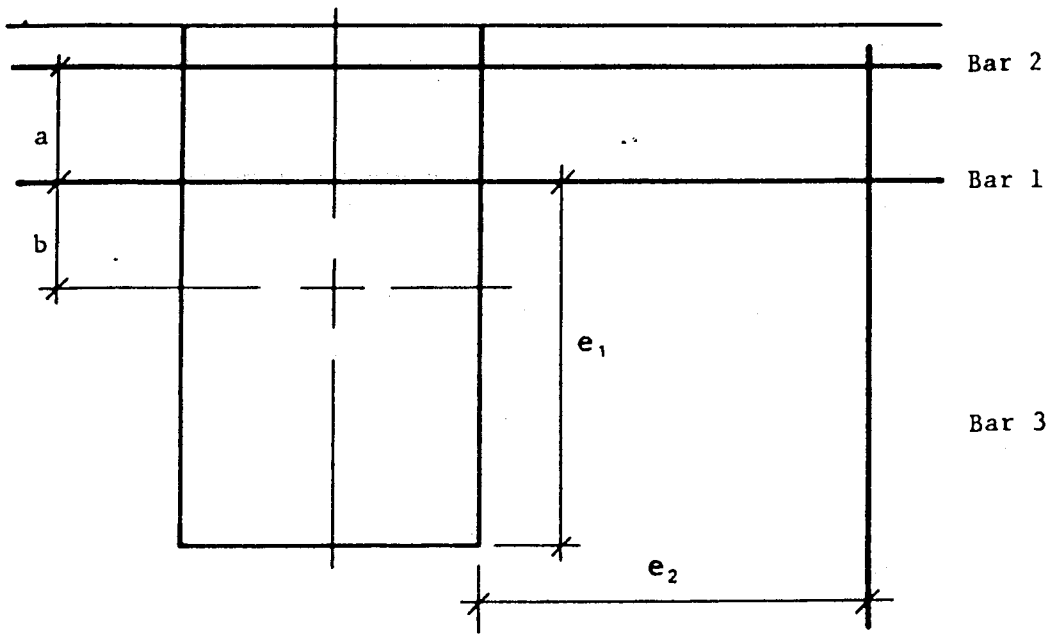

Figure 4.6 Anchoring Efficiency

Consider the arrangement shown in Figure 4.6. Bars 1 and 3 are in the top mat; bar 2 is in the bottom mat. α_1 and α_2 are the strut angles associated with bars 1 and 2 respectively.

For bar 1, a unit bar force of ΔF transferred from a shear strut to an anchoring strut produces a decrease in shear (ΔV_1) equal to:

$$\Delta V_1 = \Delta F \times \tan\alpha_1$$

The increase in moment capacity (ΔM_1) about the column centroid is equal to:

$$\Delta M_1 = \Delta F \times {}^{e_1}/_{e_2} \times 0.9 \times d_s + \Delta V_1 \times b$$

For bar 2, the corresponding decrease in net shear is:

$$\Delta V_2 = \Delta F \times \tan\alpha_2$$

and the increase in moment is:

$$\Delta M_2 = \Delta V_2 \times (a + b)$$

The ratios of incremental moment to decremental shear for the two bars are:

$$\Delta M_1 / \Delta V_1 = \frac{0.9 d_s {}^{e_1}/_{e_2}}{\tan\alpha_1} + b$$

$$\Delta M_2 / \Delta V_2 = a + b$$

The term $\frac{0.9 d_s {}^{e_1}/_{e_2}}{\tan\alpha_1}$ is the anchoring efficiency of bar 1. If it is greater than 'a', then the development of an in-plane strut will precede the uplift at bar 2.

Appendix I contains a numerical example of the construction of a complete shear-moment interaction diagram.

Chapter 5

Edge Column Tests

Forty-three individual slab-column connections from eight separate investigations are considered here. These include both single and double column tests with a wide variety of boundary conditions. The sampling, though not exhaustive, provides a diverse set of data with which to test the proposed model. The test specimens ranged in scale from ¼ to fullsize. Reinforcement details for each connection are provided in Appendix II. Table 5.1 summarizes the test results. A brief description of each test follows.

5.1 Single Column Tests

There are two types of single column test:

1. those in which loads are applied to the column and distributed by the slab to its boundaries and
2. those in which loads are applied to the slab at a fixed distance from the column.

These two testing methods are not equivalent. Although both fix the ratio of moment to shear, the second method also dictates the manner in which internal forces may be distributed through the slab. By providing only displacement control on the boundary, the first method allows the slab some freedom in determining its own force distribution along the boundary.

There are several advantages to single column tests. They are relatively inexpensive and permit testing of full

scale specimens. The experimenter has complete control over all loads and can isolate their effects.

The disadvantages to single column tests centre around a concern that they do not realistically model a slab-column connection. The effects of boundary conditions, confinement and in-plane forces are largely ignored in single column tests. Load redistribution is not possible. The importance of these effects with respect to the ultimate capacity of the connection has not been established.

5.1.1 Stamenković and Chapman

Stamenković and Chapman[19] conducted an extensive series of tests of interior, edge and corner columns under a variety of loading conditions. A schematic diagram of their apparatus for an edge column is shown in Figure 5.1. Slabs were 3 in. thick and 36 in. square. Loading was applied through the column stubs which were 5 in. square.

The boundary conditions were not well defined. The slab was supported on 16 steel tie rods which passed through the slab and were clamped in place by means of nuts. It is unclear how much rotational and lateral restraint they provided.

Six specimens were tested with moment to shear ratios ranging from zero to ∞. The geometric similarity of the specimens allows some assessment of how well the analytical model predicts the shape of the shear-moment interaction diagram. In Figure 5.2, the test results are plotted against

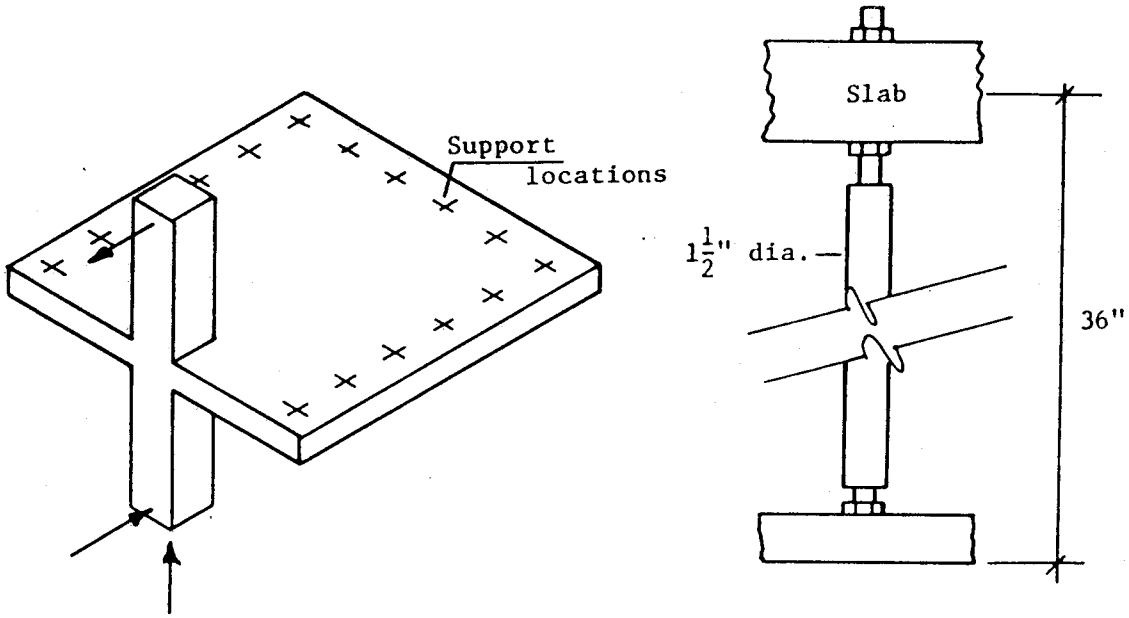

(after Stamenković and Chapman)

Figure 5.1 Stamenković and Chapman: Test Apparatus

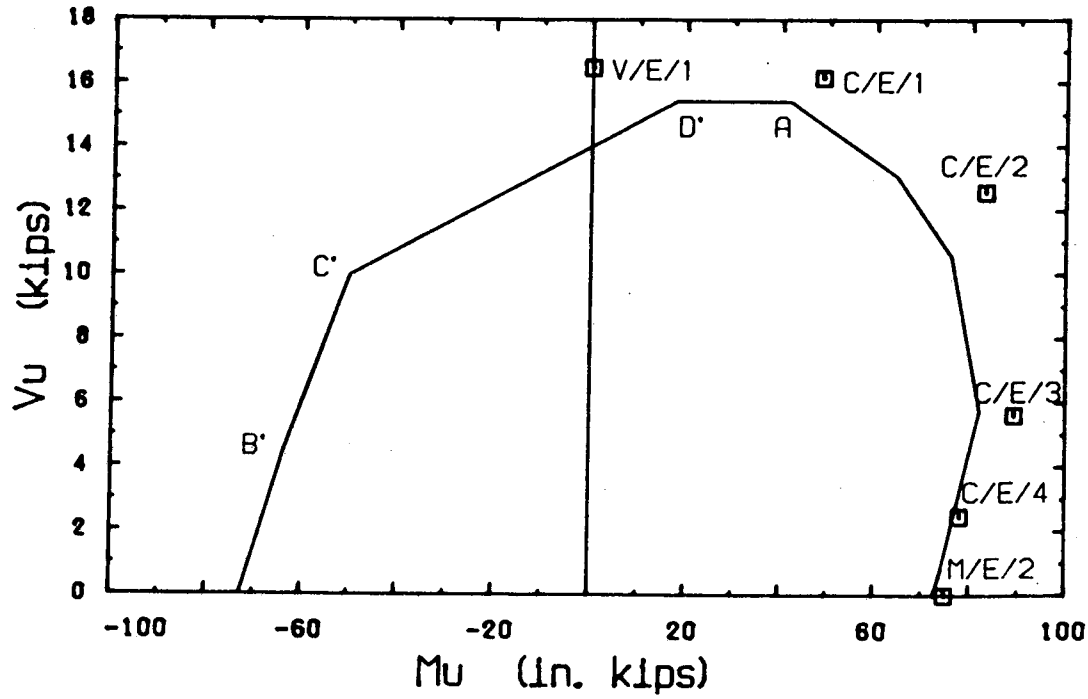

Figure 5.2 Stamenković and Chapman: Interaction Diagram

an interaction diagram which assumes a concrete cylinder strength of 4000 psi and a steel yield of 71.9 ksi. The procedure used in constructing this diagram is outlined in Appendix I.

The mechanics of the model preclude simple scaling of the test results in order to account for differences in material properties. The following procedure was used to estimate equivalent test results which would have been measured had the specimens had identical material properties. For each test, a point on the interaction diagram with the same ratio of moment to shear is found. An equivalent test result is calculated by mutilpying the values of shear and moment from the interaction diagram by the corresponding test to predicted ratio (see Tables 6.1 and 6.2).

5.1.2 Zaghlool

Zaghlool[21] conducted a series of tests concentrating on edge and corner columns. Columns ranged in size from 7 in. to 14 in. square. Edge column slabs were 38 × 72 × 6 in. As in the tests of Stamenković and Chapman, load was applied through the column stubs. Figure 5.3 shows the test set-up used. The boundaries were simply supported with uplift permitted.

A total of eight edge column tests were made. Four of these were on geometrically similar specimens under varying moment to shear ratios. In Figure 5.4, these four results

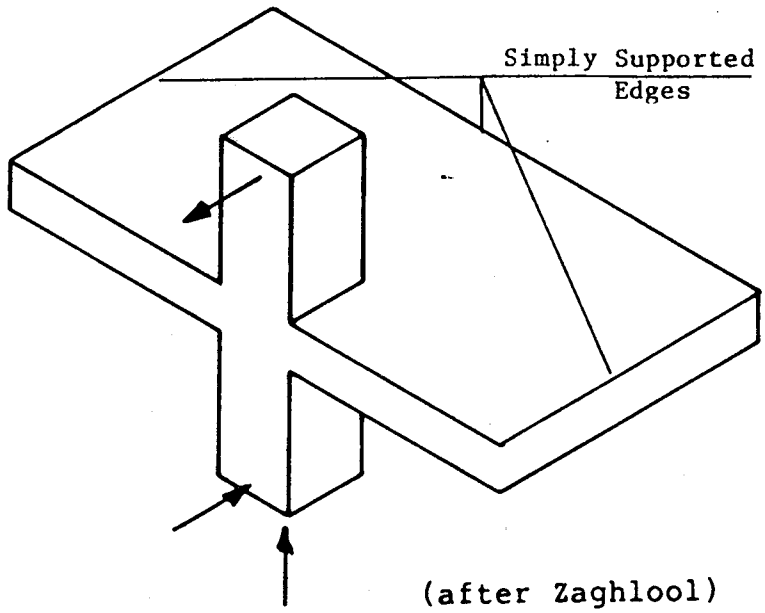

Figure 5.3 Zaghlool: Test Apparatus

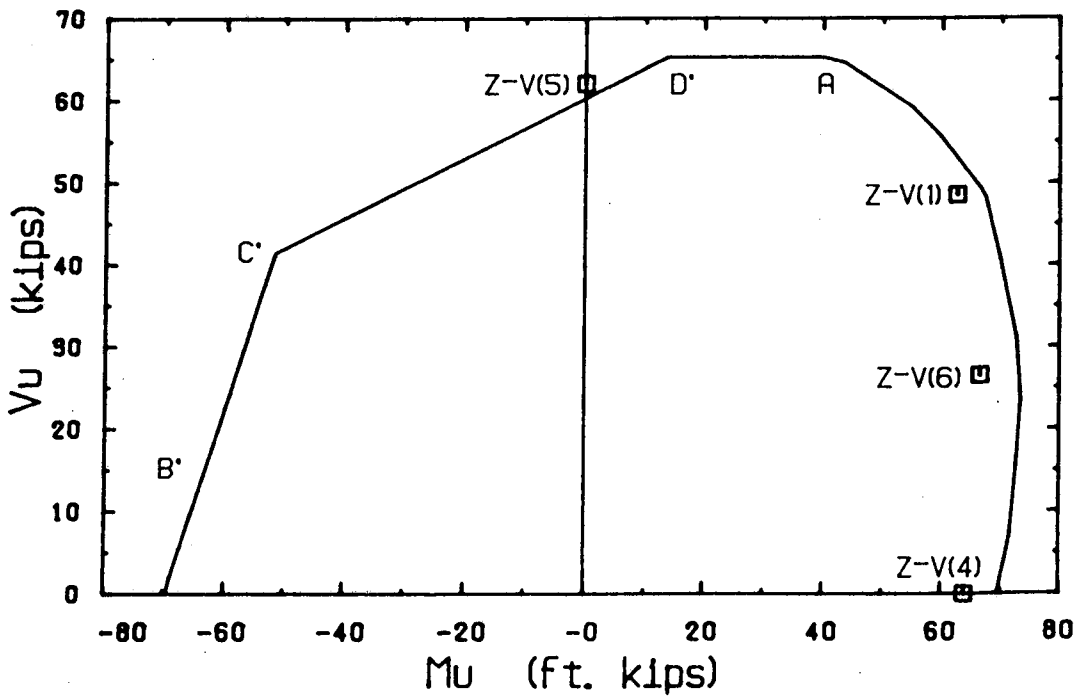

Figure 5.4 Zaghlool: Interaction Diagram

are plotted against a complete interaction based on a steel strength of 69.0 ksi and a concrete cylinder strength of 5000 psi. Test results were plotted using the same procedure that was described for those of Stamenković and Chapman.

With the remaining four specimens Zaghlool varied slab reinforcement and column size. There is some doubt as to the placement of reinforcement in test number Z-IV(4). It would appear that the high level of reinforcement in both the column and slab required that the bars actually touch. As a result, test Z-IV(1) was the most heavily reinforced of all the slab-column connections considered.

5.1.3 Kane

Kane[7] tested four specimens with rectangular columns loaded through the slab at fixed eccentricities. Slabs were approximately 700 × 400 × 50 mm. His test set-up is shown in Figure 5.5. In each test, 60% of the load was eccentric to the centreline of the column. The principal variable was the distribution of the reinforcement.

5.1.4 Hanson and Hanson

Hanson and Hanson[3] tested one edge column specimen (illustrated in Figure 5.6). The column was 6 in. square and the slab dimensions were 48 × 45 × 3 in. A single line load was applied to the specimen by means of a steel beam bearing on the slab. The stiffness of the steel section probably had the effect of reducing the two-way action of the slab.

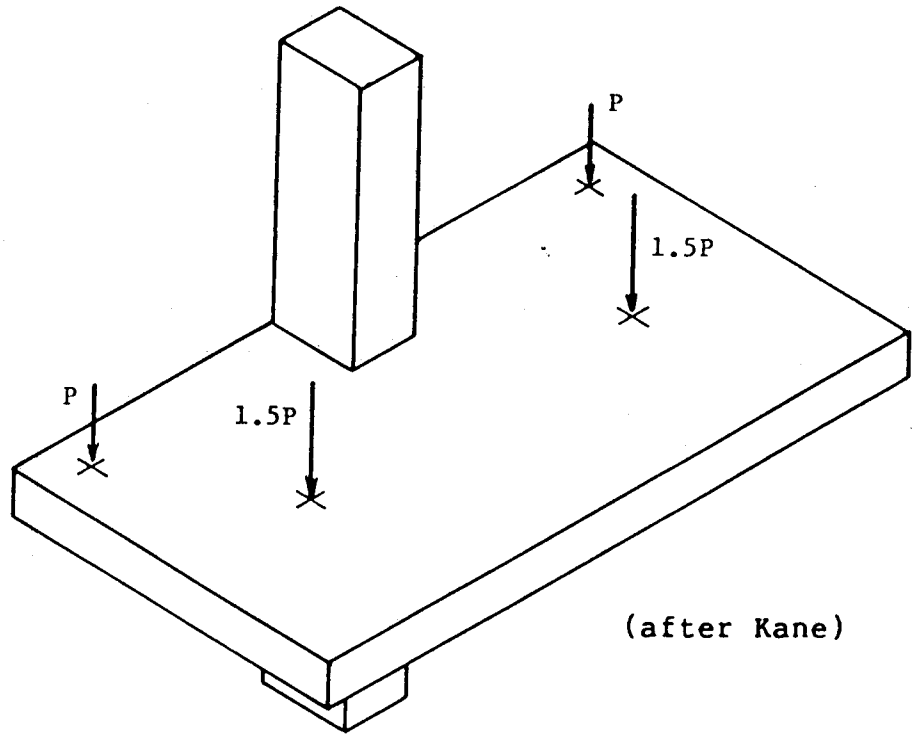

Figure 5.5 Kane: Test Apparatus

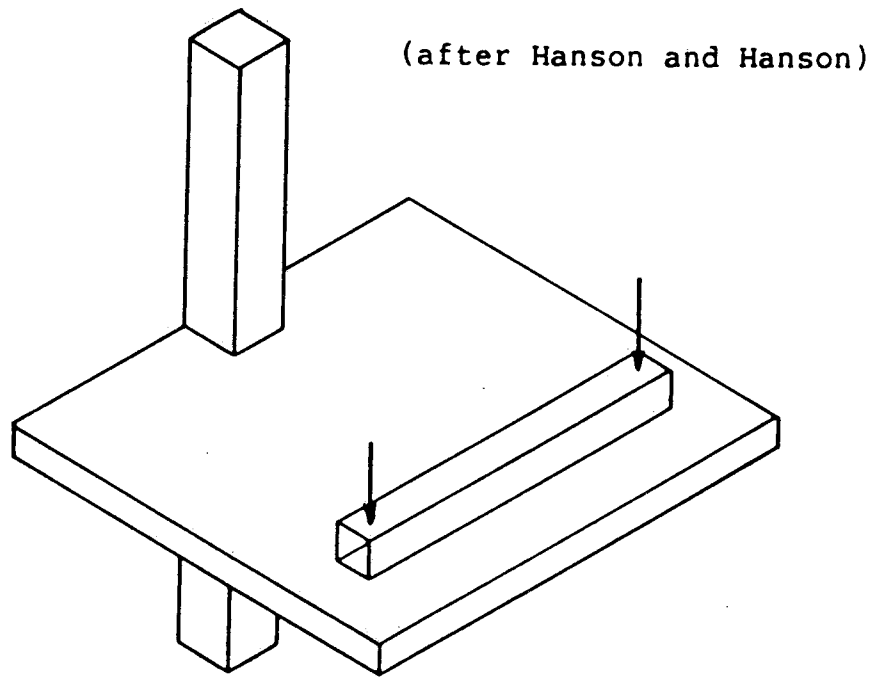

Figure 5.6 Hanson and Hanson: Test Apparatus

5.2 Double Column Tests

Several investigators have been concerned that the effects of in-plane forces, boundary conditions, confinement and load redistribution might be so significant as to invalidate the single column test. Although double column tests may be an improvement in modelling over the single column tests, there remains the problem of separating the above effects so that they may be included in analysis.

5.2.1 Regan

Regan[13] conducted an extensive test program which included interior, edge and corner columns plus wall supported slabs. His test apparatus for edge columns SE1 through SE8 is shown in Figure 5.7. Specimens SE9, SE10 and SE11 were larger with 10 loading points instead of 8. All slabs were 125 mm thick. Variables included distribution of reinforcement, column aspect ratio and column size. Specimen SE3 is excluded from this presentation since it contained shear reinforcement.

A unique feature of these tests was the absence of any bottom reinforcement parallel to the free edge. Also of interest are the low values for ρ_{sv}^{T1} in tests SE2, SE6 and SE9 through SE11. While all tests were described as having punching failures, SE2 and SE9 through SE11 were said to have a strong flexural influence. This is interpreted as meaning that the slab showed considerable distress prior to failure.

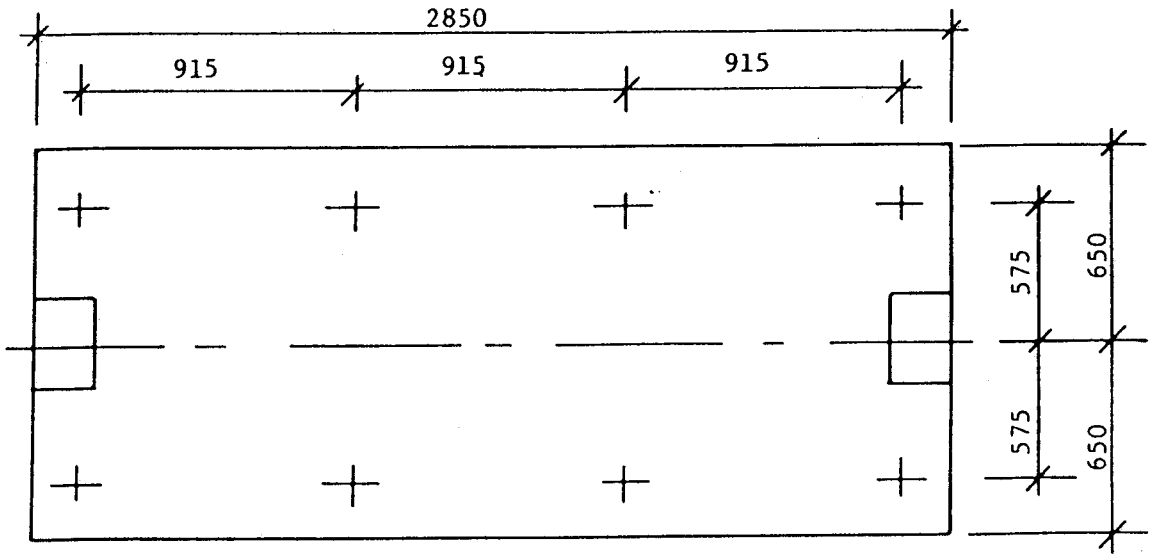

(after Regan)

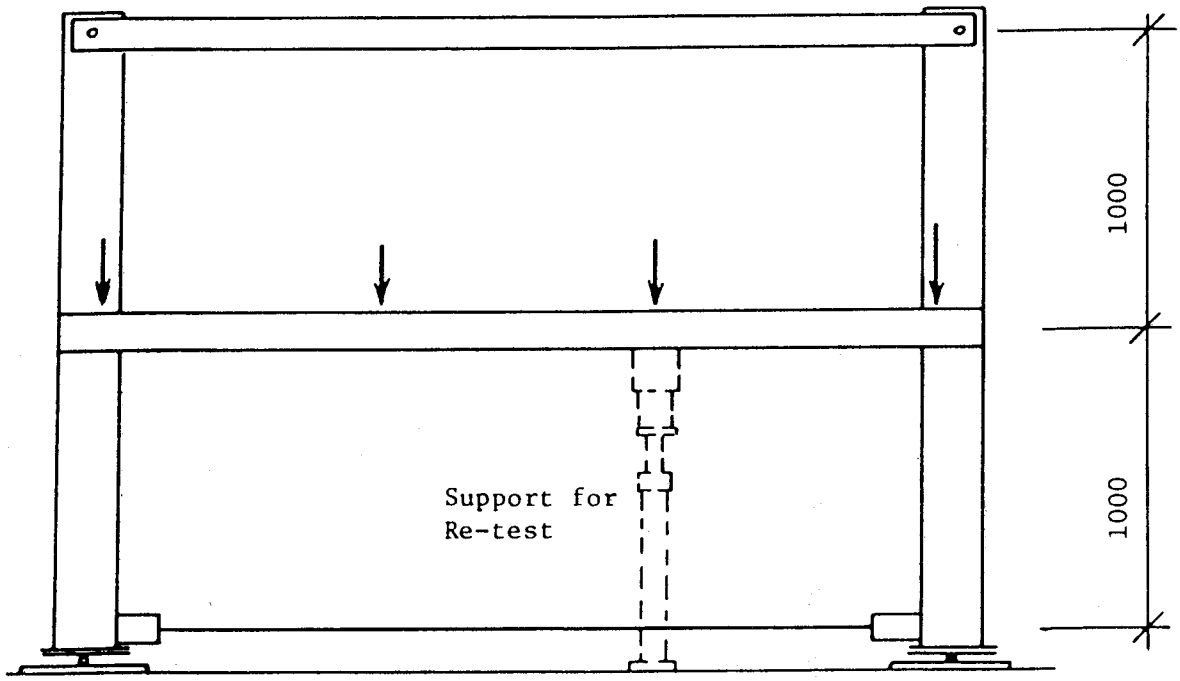

Figure 5.7 Regan: Test Apparatus

In those cases where the unfailed end of the specimen appeared to be in good condition, a re-test was performed. This consisted of supporting the slab at an intermediate point and loading the intact column to failure. For these tests, the restraint afforded by the previously failed connection was negligible so the unbalanced moment was taken to be zero.

5.2.2 Scavuzzo, Gosselin and Lamb

Scavuzzo, Gosselin and Lamb[16, 8, 2] each tested four specimens with essentially identical loading and support conditions (illustrated in Figure 5.8). All slabs were 63 mm (2.5 in.) thick. Specimens were subjected to cycles of both gravity and lateral loads prior to being failed under gravity load only. To model slab continuity, rotations on the long side edges were restrained by means of attaching steel hollow sections. These hollow sections projected below the plane of the slab. Each was tied to its counterpart on the other side of the slab. In order for this procedure to prevent edge rotations, an in-plane tensile force of unknown magnitude is induced in the slab.

The primary objective of these three investigations was to examine the frame action of a slab-column system. Deflections, rotations and moment and shear distributions under service loads were paramount. Ultimate capacities were of secondary importance. As a result, the actual failure loads of some specimens were not recorded. For these cases,

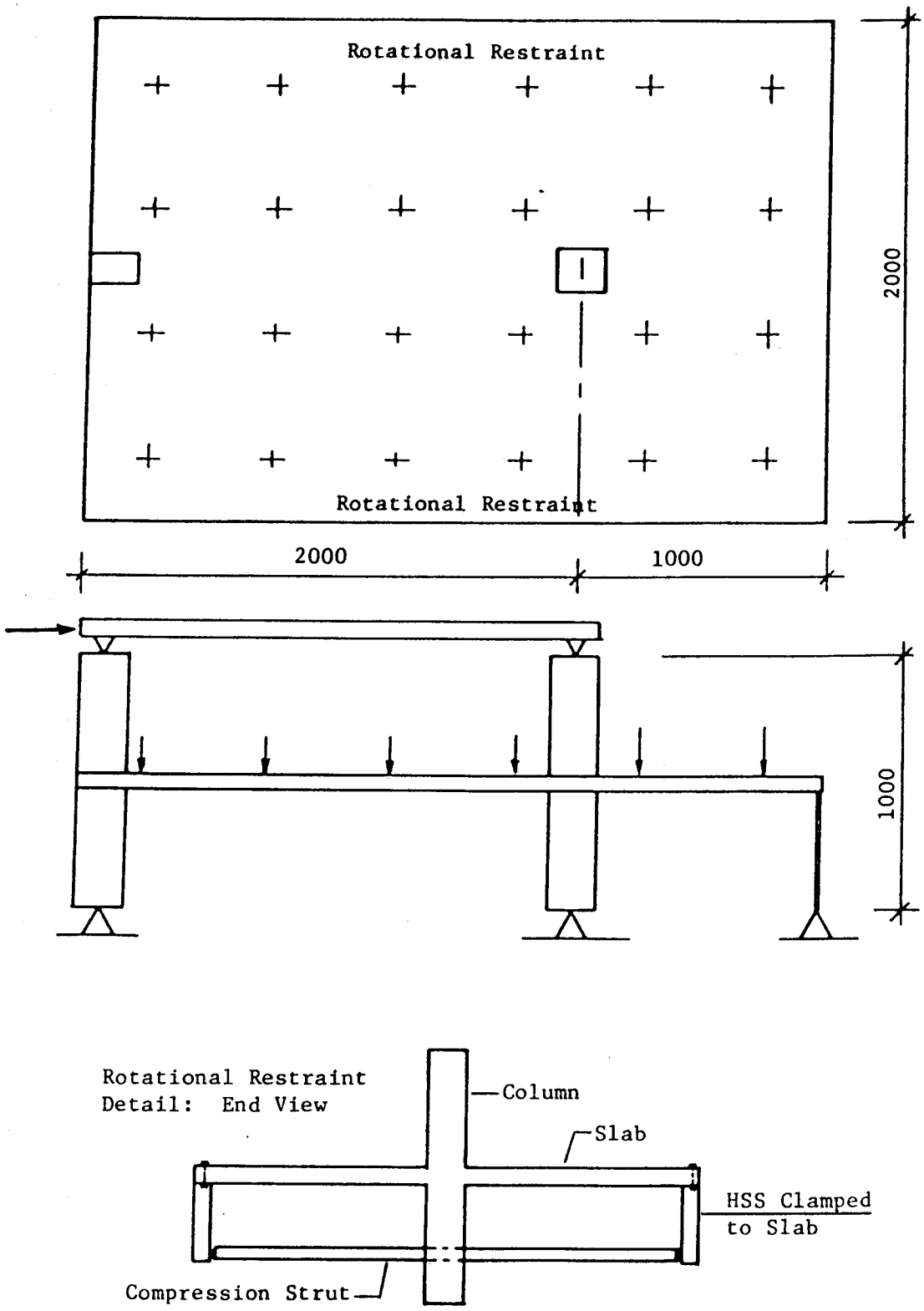

(after Scavuzzo, Gosselin and Lamb)

Figure 5.8 Scavuzzo, Gosselin and Lamb: Test Apparatus

the last reported shear and moment values along with the approximate percentage of ultimate load are given in Table 5.1.

5.2.2.1 Scavuzzo

Only test S-1 by Scavuzzo is included in this paper. Tests S-2, S-3 and S-4 by Scavuzzo all contained some form of shear reinforcement. Test S-1 was described as having a punching failure.

It is interesting to note that shear reinforcement did not appear to increase the ultimate capacities of the specimens. All four specimens failed at nearly identical shears and moments. However, the post-failure capacities of the shear reinforced specimens were greatly enhanced. The difference in post-failure behavior between Scavuzzo's test S-1 and his tests S-2, S-3 and S-4 is analagous to that between tied and spiral columns.

5.2.2.2 Lamb

Of the four tests conducted by Lamb, two (L-3 and L-4) had edge beams and are therefore excluded from this investigation. Specimens L-1 and L-2 each had the same extremely light reinforcement layout.

Although specimen L-1 was described as having a punching failure at the edge column location, this was preceded by extensive cracking in the slab. Specimen L-2 failed by punching at the interior column but Lamb felt that the condition of the slab at the edge column indicated near

failure.

5.2.2.3 Gosselin

Gosselin tested four specimens with drop panels, accounting for his larger values of t in Table 5.1. Reinforcement patterns and drop panel dimensions were the major variables. Two of the specimens (G-3 and G-4) failed by punching at the interior column. Since there was no indication that the edge column regions were near ultimate, these two tests have been excluded from this investigation.

Tests G-1 and G-2 each failed at the edge column. Specimen G-1 had a punching failure accompanied by considerable cracking of concrete and yielding of steel. Specimen G-2 was described as having a rotational failure. This also involved extensive cracking and yielding but there was no clearly defined punching failure surface.

Table 5.1 Summary of Test Results

Investigator	Mark	t	c_1	c_2	f'_c	fy	V_u	M_u	% ult.
Stamenkovic and Chapman (19)	V/E/1	3.0 in.	5.0 in.	5.0 in.	4225 psi	71.9 ksi	16.80 kips	-	100
	C/E/1	"	"	"	4570 psi	65.0 ksi	16.45 kips	49.5 in.kips	"
	C/E/2	"	"	"	4780 psi	71.9 ksi	12.30 kips	81.2 in.kips	"
	C/E/3	"	"	"	4930 psi	"	5.60 kips	89.0 in.kips	"
	C/E/4	"	"	"	4030 psi	"	2.46 kips	78.2 in.kips	"
	M/E/2	"	"	"	3870 psi	"	-	74.0 in.kips	"
Kane (7)	K-1	51 mm	100 mm	68 mm	30.2 MPa	480 MPa	24.0 kN	2.38 kN m	"
	K-2	48 mm	114 mm	75 mm	35.9 MPa	"	20.9 kN	2.07 kN m	"
	K-3	48 mm	114 mm	75 mm	41.2 MPa	"	25.1 kN	2.48 kN m	"
	K-4	48 mm	114 mm	75 mm	27.6 MPa	"	18.2 kN	1.80 kN m	"
Zaghlool (21)	Z-IV(1)	6.0 in.	7.0 in.	7.0 in.	3965 psi	69.0 ksi	27.5 kips	33.2 ft.kips	"
	Z-V(1)	6.0 in.	10.5 in.	10.5 in.	4980 psi	68.7 ksi	48.4 kips	62.4 ft.kips	"
	Z-V(2)	6.0 in.	10.5 in.	10.5 in.	5870 psi	68.7 ksi	55.5 kips	69.0 ft.kips	"
	Z-V(3)	6.0 in.	10.5 in.	10.5 in.	5620 psi	68.9 ksi	60.3 kips	76.4 ft.kips	"
	Z-V(4)	6.0 in.	10.5 in.	10.5 in.	5080 psi	63.4 ksi	-	60.0 ft.kips	"
	Z-V(5)	6.0 in.	10.5 in.	10.5 in.	5100 psi	69.0 ksi	62.8 kips	-	"
	Z-V(6)	6.0 in.	10.5 in.	10.5 in.	4540 psi	69.1 ksi	26.3 kips	65.0 ft.kips	"
	Z-VI(1)	6.0 in.	14.0 in.	14.0 in.	3770 psi	69.0 ksi	59.6 kips	78.8 ft.kips	"
Lamb (8)	L-1	63 mm	225 mm	150 mm	34.7 MPa	395 MPa	27.6 kN	3.49 kN m	86
	L-2	"	"	"	43.8 MPa	"	30.7 kN	5.12 kN m	92
Gosselin (2)	G-1	79 mm	"	"	38.1 MPa	375 MPa	38.0 kN	7.23 kN m	85
	G-2	95 mm	"	"	39.0 MPa	"	43.6 kN	11.16 kN m	83

Table 5.1 Continued

Investigator	Mark	t	c_1	c_2	f'_c	fy	V_u	M_u	% ult.
Regan (14)	SE1	125 mm	300 mm	200 mm	35.5 MPa	480 MPa	198. kN	39.5 kN m	100
	SE2	"	"	"	44.4 MPa	"	192. kN	34.0 kN m	"
	SE4	"	200 mm	300 mm	26.6 MPa	"	152. kN	30.5 kN m	"
	SE5	"	"	"	44.9 MPa	"	164. kN	38.5 kN m	"
	SE6	"	"	"	32.9 MPa	490 MPa	149. kN	27.5 kN m	"
	SE7	"	"	"	39.8 MPa	"	129. kN	31.7 kN m	"
	SE8	"	300 mm	100 mm	42.1 MPa	480 MPa	136. kN	33.7 kN m	"
	SE9	"	250 mm	250 mm	41.9 MPa	"	123. kN	35.7 kN m	"
	SE10	"	"	"	41.1 MPa	"	114. kN	36.0 kN m	"
	SE11	"	"	"	51.5 MPa	"	138. kN	39.5 kN m	"
	SE1(R)	125 mm	300 mm	200 mm	35.5 MPa	480 MPa	233. kN	-	"
	SE2(R)	"	"	"	44.4 MPa	"	205. kN	-	"
	SE5(R)	"	"	"	44.9 MPa	"	189. kN	-	"
	SE6(R)	"	"	"	32.9 MPa	490 MPa	163. kN	-	"
	SE7(R)	"	"	"	39.8 MPa	"	125. kN	-	"
	SE8(R)	"	300 mm	100 mm	42.1 MPa	480 MPa	173. kN	-	"
	SE9(R)	"	250 mm	250 mm	41.9 MPa	"	142. kN	-	"
	SE10(R)	"	"	"	41.1 MPa	"	151. kN	-	"
	SE11(R)	"	"	"	51.5 MPa	"	154. kN	-	"
Scavuzzo (16)	S-1	2.5 in.	6.0 in.	4.0 in.	5530 psi	55 ksi	7.22 kips	41.2 in.kips	"
Hanson & Hanson (3)	D15	3.0 in.	6.0 in.	6.0 in.	4510 psi	53 ksi	2.71 kips	93.0 in.kips	"

Chapter 6

Discussion of Results

6.1 Accuracy

The usual measure of accuracy for an analytical model is the ratio of test to predicted result. However, Van Dusen states that an analytical model should not be judged solely upon the quality of test to predicted ratios. A good model should also provide an understanding of the mechanisms at work and be able to predict the behavior of a specimen under a wide range of conditions.

One of the reasons for selecting the truss model in the first place was that it predicted both the pattern of concrete cracking and the shape of the failure surface. Furthermore, the mechanism developed for the failure of a shear strut, namely the pushing of the tension mat of reinforcement out of the plane of the slab, is in agreement with observations of test specimens.

With the above comments in mind, consider the test to predicted ratios listed in Tables 6.1. and 6.2. The tests have been divided into two categories:

1. zero moment tests (vertical load only) and
2. shear-moment tests (unbalanced moment present).

Table 6.1 Summary of Analytical Results: Zero Moment Tests

Ref.	Mark	Test/Pred	ρ_{sv}^{T} (%)	$\rho_{sv}^{T} \times f_y/f'_c$
19	V/E/1	1.18	1.44	0.245
21	Z-V(5)	1.03	2.00	0.271
13	SE1(R)	1.10	1.30	0.176
	SE2(R)	1.23	0.90	0.097
	SE5(R)	1.28	1.22	0.130
	SE6(R)	1.17	0.94	0.140
	SE7(R)	0.91	1.15	0.142
	SE8(R)	1.09	1.25	0.143
	SE9(R)	0.98	0.91	0.104
	SE10(R)	1.05	0.91	0.106
	SE11(R)	1.00	0.91	0.085

Table 6.2 Summary of Analytical Results: Shear-Moment Tests

Ref.	Mark	Test/Pred	ρ_{sv}^{T1} (%)	$\rho_{sv}^{T1} \times f_y/f'_c$	f_u/f_y
21	Z-IV(1)	0.68	3.19	0.556	-
	Z-V(1)	0.96	2.13	0.294	-
	Z-V(2)	0.97	2.44	0.285	-
	Z-V(3)	1.04	2.47	0.303	-
	Z-V(4)	0.92	2.13	0.266	-
	Z-V(6)	0.90	2.13	0.324	-
	Z-VI(1)	1.10	1.60	0.292	-
3	D15	0.90	2.18	0.256	-

Table 6.2 Continued

Ref.	Mark	Test/Pred	ρ_{sv}^{T1} (%)	$\rho_{sv}^{T1} \times f_y/f'_c$	f_u/f_y
19	C/E/1	1.09	1.52	0.216	-
	C/E/2	1.12	1.52	0.289	-
	C/E/3	1.10	1.52	0.275	-
	C/E/4	1.02	1.52	0.271	-
	M/E/2	1.02	1.52	0.282	-
7	K-1	1.02	2.03	0.323	-
	K-2	0.94	1.99	0.266	-
	K-3	1.03	1.99	0.231	-
	K-4	0.92	1.99	0.345	-
14	SE1	0.99	1.72	0.232	1.59
	SE2	1.48	0.25	0.027	1.52
	SE4	0.95	1.54	0.278	1.59
	SE5	1.05	1.22	0.130	1.59
	SE6	1.13	0.66	0.100	1.61
	SE7	0.90	1.14	0.143	1.61
	SE8	0.84	1.81	0.207	1.59
	SE9	1.20	0.68	0.078	1.59
	SE10	1.23	0.68	0.079	1.59
	SE11	1.31	0.68	0.063	1.59
16	S-1	1.04	1.03	0.102	1.44
8	L-1 (86%)	0.98	0.35	0.040	1.45
	L-2 (92%)	1.20	0.35	0.032	1.45
2	G-1 (85%)	1.11	0.47	0.046	1.43
	G-2 (83%)	1.15	0.67	0.064	1.43

6.1.1 Zero Moment Tests

In order to assess the quality of test to predicted results, the zero moment tests should be considered separately because the accuracy of predictions for these tests depends upon how well the capacity of the inverted shear strut can be estimated. The results of this investigation were obtained by assuming that the shear and shear moment capacities of control points A and A' are maintained at their adjacent inverted shear stages (control points D' and D respectively). Test to predicted ratios for zero moment tests range from 0.91 to 1.28 with an average of 1.09 and a standard deviation of 0.11, suggesting that the capacity of the inverted shear strut was underestimated.

6.1.2 Shear-Moment Tests

For the shear-moment tests, the capacities predicted by the truss model are generally in good agreement with test results. Test to predicted ratios for 23 tests, from a total number of 32, lie between 0.84 and 1.13. The 9 remaining specimens include 2 each by Lamb and Gosselin, 4 by Regan and 1 by Zaghlool. For the tests by Lamb and Gosselin, exact test to predicted values cannot be calculated since ultimate loads were not reported. It is safe to say that the true test to predicted ratios for these 4 tests should be considerably greater than those reported in Table 6.2, which means that the truss model gives very conservative estimates of ultimate strength for these specimens. As well, Regan's

SE2, SE9, SE10 and SE11 all had failure loads well in excess of that predicted. Zaghlool's Z-IV(1), however, failed at only 68% of its predicted capacity. It will be seen that these apparent aberrations can not only be explained but they in fact support the validity of the truss model.

6.1.3 Density of Reinforcement

The accuracy of results predicted by the truss model is expected to depend on the density of reinforcement for three reasons.

1. The true value of the flexural moment arm (jd) changes with variations in the reinforcing ratio. Since the model assumes a constant j equal to 0.9, predictions should overestimate heavily reinforced and underestimate lightly reinforced test specimen capacities.
2. Extremely light reinforcement may allow the steel to strain harden. While this presents no conceptual problem for the model, there is some difficulty in assessing the degree of strain hardening. Neglecting it should lead to conservative predictions for lightly reinforced specimens.
3. Heavy reinforcement would cause a compression failure of the concrete strut before the steel reaches yield. This would result in test to predicted ratios less than 1.0.

A term ρ_{sv} is used to describe the density of shear steel. In general, ρ_{sv} is equal to the ratio of the area of shear steel to the product of the perimeter of the

slab-column junction and the effective depth of the slab. In order to describe the density of reinforcement on any particular column face, the same superscripts that are used for A_{sv} are applied to ρ_{sv} so that:

$$\rho_{sv}^{T1} = \frac{A_{sv}^{T1}}{c_2 \times d_s}$$

where c_2 is the column dimension parallel to the free edge. Values of ρ_{sv} may be multiplied by the ratio of f_y to f'_c to provide a reinforcing index for shear.

For the zero moment tests, values of ρ_{sv}^{T} and $\rho_{sv}^{T} \times f_y/f'_c$ are given. Although they provide some indication as to how heavily a connection was reinforced, no real relationship between either of these two parameters and test to predicted ratios is suggested. The capacity of gravity inverted shear struts is at least partly dependent on A_{sv}^{B1} but the term ρ_{sv}^{T} does not account for this.

For the shear-moment tests, it is felt that the conditions at the front face of the column are paramount in determining the behavior of the connection. Therefore, the term ρ_{sv}^{T1} is used to estimate the governing density of reinforcement for these tests.

Figures 6.1(a) and 6.1(b) plot test to predicted ratios against ρ_{sv}^{T1} expressed as a percentage and the reinforcing index based on ρ_{sv}^{T1} repectively. The results of Lamb and Gosselin are not included since failure shears and moments for these tests were not provided.

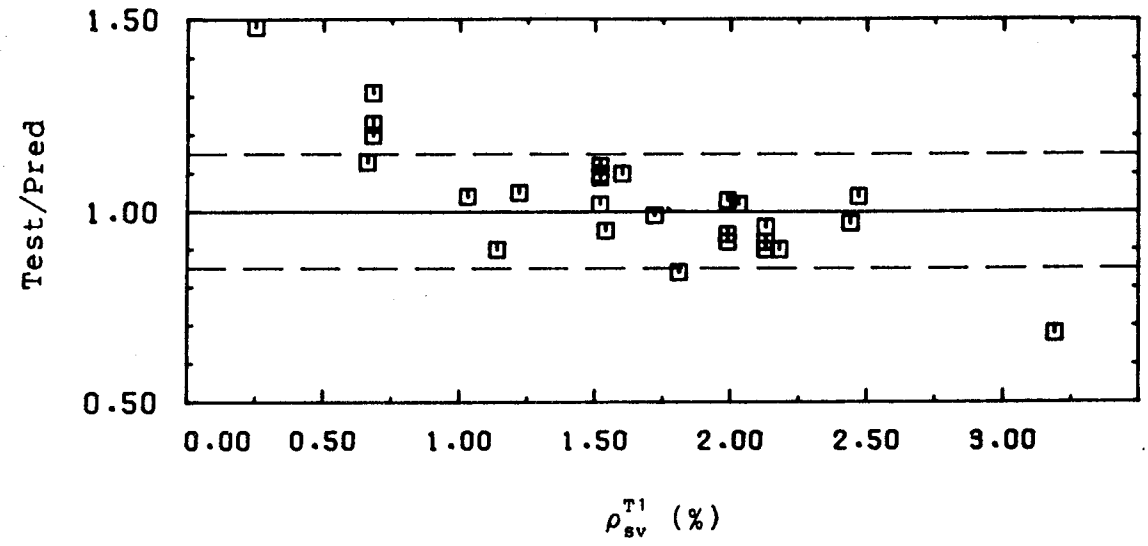

(a)

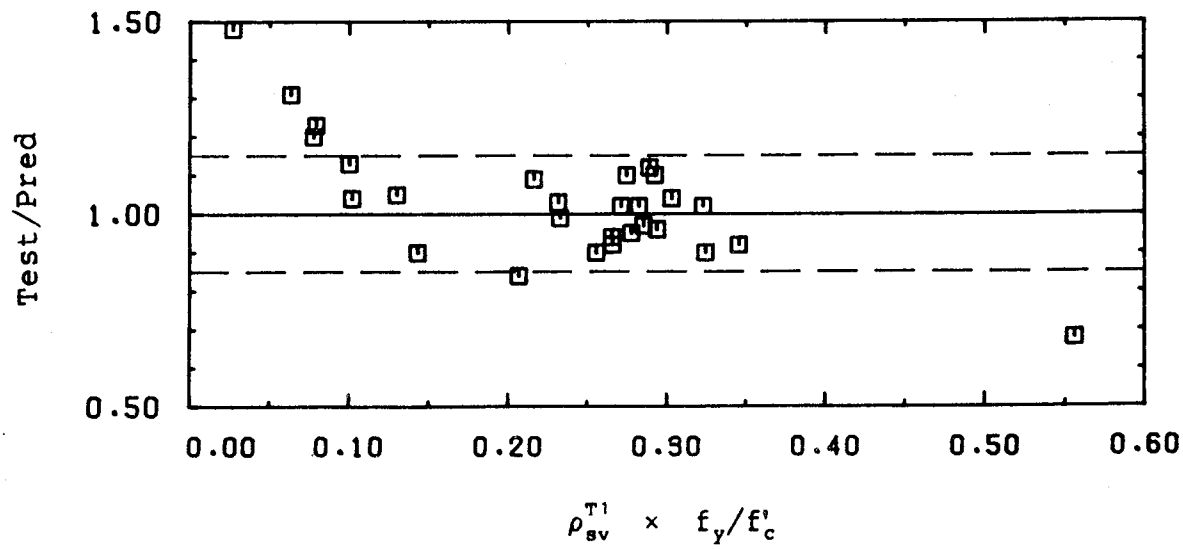

(b)

Figure 6.1 Effect of Reinforcement Density

Both plots show essentially the same trends. For values of ρ_{sv}^{T1} between about 1.0% and 2.5% (shear reinforcing index between 0.1 and 0.4) the truss model gives excellent predictions of test results. However, for ρ_{sv}^{T1} less than 0.7% (index less than 0.1), test to predicted ratios are significantly greater than 1. In addition, for test Z-IV(1) where ρ_{sv}^{T1} exceeds 3.0% (index exceeds 0.55), the model overestimates ultimate capacity by a wide margin.

For the lightly reinforced specimens, the most probable cause of enhanced ultimate capacities is strain hardening of the steel. Failure descriptions for all of these tests indicate extensive cracking and deformations of the specimen. Yielding of steel passing through the column was recorded at relatively low levels of load. All of this is consistent with strain hardening of the reinforcement and it can be seen from the ratios of f_u to f_y in Table 6.2 that the steel had sufficient post-yield strength to account for the increased test to predicted ratios.

The unconservative prediction in the case of the heavily reinforced specimen is believed to be a result of compression failure of the concrete. This would place an upper limit on ρ_{sv}^{T1} in the order of 3% for connections under combined shear and moment. The corresponding reinforcement index would be somewhere between 0.4 and 0.5. At this reinforcing density, failure is caused by crushing of the concrete. The confinement failure mode no longer governs. Although some criteria for analyzing a compression failure

could be developed, the required density of reinforcement is outside the practical limits for flat slabs, as was anticipated in the preliminary assumptions in Chapter 3.

The model assumes that the steel stress at failure is equal to the yield stress. Figure 6.1(b) clearly indicates the tests for which this assumption was not accurate. Those with reinforcing indices less than 0.10 (tests SE2, SE9, SE10 and SE11) had steel stresses at failure exceeding yield. For these lightly reinforced specimens, there is a marked correlation between reinforcing index and test to predicted ratio. Although exact values of test to predicted ratios cannot be calculated, the tests of Lamb and Gosselin appear to confirm to this trend as well.

A statistical measure of the accuracy of the model should be based only on those shear-moment tests in which strain hardening of the reinforcement or compression failure of the concrete was not a factor. Therefore, tests SE2, SE9, SE10, SE11, L-1, L-2, G-1, G-2 and Z-IV(1) should be excluded from the sample. For the remaining 23 tests, the model must yield accurate predictions if it is to be deemed valid. For this sample, the average test to predicted ratio is 1.00 and the standard deviation is 0.081.

6.2 Classification of Failure

Regan[12] stated that the failure of a slab-column connection is not easily categorized as either shear (punching) or flexural. He summarized prevailing thought by

describing some failures as undeniably shear dominated and others as essentially flexural with punching occurring as a secondary phenomenon. In support of this, he presented a series of load deflection diagrams ranging from highly ductile, folding failures of a slab to brittle punching failures.

The categories of shear and flexural failure modes are misleading. A better system of classification would be to consider local connection failures as opposed to overall slab failures. Both types of structural collapse may be either ductile or non-ductile.

Folding failures of the slab occur when the strength of the slab-column connection exceeds the capacity of the slab to deliver load to the connection. Techniques such as yield line analysis already exist for describing this type of failure. Local connection failures are distinct from overall slab failures in that they involve the breaking away of the column and a portion of slab from the rest of the slab. Although they are not part of the same classification as slab failures, it is not hard to imagine cases in which the overall slab strength and the local connection strength are so close that it is hard to distinguish the actual failure mode. Nevertheless, the ultimate load of a test specimen is governed by the lesser of these two independent failure capacities, namely the slab strength or the connection strength.

6.3 Ductility

Ductility at ultimate is not as easily predicted for a slab-column connection as it is for a beam. Yielding of reinforcement, usually considered synonymous with ductile behavior in reinforced concrete, is common in the vicinity of the column and yet failure may be described as sudden and non-ductile. Conversely, the punching mode of failure cannot be viewed as inherently non-ductile since it frequently occurs after extensive cracking and deformations. The truss model suggests a solution to this paradox since it makes yielding of the reinforcement and the punching mode of failure compatible. Although yielding of the reinforcement is necessary for ductility, the mechanism of failure is at least as important.

The interaction diagram describes a series of different failure mechanisms. The amount of reinforcement needed to cause a non-ductile failure may change depending upon which mechanisms dominate. In the vicinity of control points B and B', the slab undergoes extreme rotations with respect to the column. Shear struts of opposite orientation are adjacent to each other while in-plane strut development is maximum, suggesting large strain discontinuities. These circumstances are conducive to extensive cracking in the slab prior to failure. Conversely, near control points A and A', the rotation between the slab and the column is near zero. Shear strut are all of the same orientation, leading to a classic punching type failure with limited cracking.

6.4 Material Properties

In Chapter 3, it was suggested that the tensile strength of the concrete was probably more relevant than the compressive strength in determining the strut angle. The term $\sqrt{f'_c}$, which is generally considered proportional to the tensile strength, was used to calibrate α. This indirect approach limits the application of the calibration to cases of normal weight concrete which have not had their tensile strengths enhanced by additives. This is an unnecessary limitation which could be avoided by using some tensile strength measure for the concrete (say split cylinder) in lieu of $\sqrt{f'_c}$. Unfortunately, most of the tests used to calibrate α in this investigation did not report tensile strengths of the concrete.

All reinforcing steel used in the test specimens included here had reasonably well defined yield plateaus. The effects of using strain hardened reinforcement such as cold drawn wire are not known.

6.5 Scale Effects

Several investigators have attempted to evaluate the effects of using small scale specimens. Some have argued that if scaled specimens are used, then material properties (in particular, concrete strengths) should be based on similarly scaled samples.

There are two objections to this line of reasoning. First, it is believed that one of the main factors which

contribute to the scale effect in compression strength tests is the lateral end confinement provided by friction between the cylinder or cube and the testing machine. This frictional restraint is not a factor in the testing of a slab-column connection. Secondly, the scale effects for compression tests disappear for specimens over a certain size. Therefore, even if scale effects could be accounted for with scaled down compression tests, it is not possible to determine which size of cylinder or cube should be used. This is because 'scale' is not an absolute measure. A ¼ scale model may still be large enough so that its material properties show no scale effect.

In this investigation, the 150mm by 300mm cylinder test (f'_c) is taken as the standard for concrete strength. For those tests in which concrete strengths were based on cube tests (f_{cu}), the following equations were used to provide equivalent cylinder strengths. The first expression, suggested by l'Hermite and reported by Neville[11], gives the ratio of f'_c to 150 mm cube strength. The second equation accounts for the effect of using a 100 mm cube instead of a 150 mm cube. It is based on Figure 8.19 of Neville's book.

$$\frac{f'_c}{f_{cu150}} = 0.76 + 0.2\log_{10}\frac{f_{cu150}}{2840} \qquad (f_{cu150} \text{ in psi})$$

$$f_{cu150} = \frac{f_{cu100}}{1.04}$$

6.6 Boundary Conditions and In-Plane Forces

Despite a wide range in boundary conditions and in-plane forces in the shear-moment tests, the truss model maintains a high degree of accuracy. This suggests that, for these tests, the slab boundaries were far enough removed from the failure regions so as not to affect the ultimate behavior. Therefore, because of their greater flexibility in controling loads and improved economy, single column tests may be better than double column tests for the purpose of evaluating the ultimate capacity of a slab-column connection.

In-plane forces were certainly present in all double column tests although their magnitudes were not always reported. It is possible that, for the more lightly reinforced specimens, in-plane forces played a proportionately greater role at ultimate and are partly responsible for the increased capacities of these specimens. However, it appears that for most specimens, their effects were small enough to be neglected at ultimate.

Ultimate capacity, however, is not the only quantity significant to design. A fundamental question, beyond the scope of this investigation, is what ratio of moment to shear is actually present in a slab-column connection just prior to collapse. This question cannot be addressed without accounting for moment redistribution. Likewise, load-deflection characteristics are expected to be highly dependent on boundary conditions and in-plane forces. None

of these problems can be realistically examined with single column tests.

6.7 Aspects of Testing

The mechanisms of the proposed truss model require a re-examination of experimental procedures. The importance of providing exact information regarding placement of reinforcement is highlighted. Average reinforcing ratios taken across large sections of slab are not relevant to a highly localized connection failure.

The model attaches much greater significance to the parameter d'. Unless extreme care is taken when placing reinforcement, small absolute variations in d' will produce large percentage errors. This is especially critical for small scale specimens.

The position of load application is significant to the failure capacity of the specimen. If a loading point is close enough to the column, it will enhance the strength of the shear struts by providing confinement to the out-of-plane forces. It is necessary to remove this load effect in order to assess the strength of the connection alone.

6.8 Further Applications of Model

6.8.1 Generalization of Model

The most obvious extensions to the proposed model would be the treatment of interior and corner columns. In fact, by virtue of the technique used to calibrate the model, interior columns under balanced moment have already been dealt with. It is felt that neither corner columns nor interior columns under unbalanced moment will present any major difficulties. Two other extensions will be required before the model can be transformed into a design procedure.

The first of these is the treatment of slabs with holes. Depending upon their location and size, slab holes can have two effects. Holes close to the column reduce the area of concrete available to carry compression. This may increase the density of shear reinforcement sufficiently to cause a compression failure. The model treats this problem by maintaining limits on ρ_{sv}. Holes which are farther from the column reduce the area of concrete available for confinement of out-of-plane forces. This can be accounted for by altering the effective tributary width (s_{eff}) of the affected bars.

Another important extension will be the treatment of shear reinforcement and concretes with enhanced tensile strength. Shear reinforcement presents no conceptual hurdle for the model. It provides additional confinement for out-of-plane forces. However, there may be problems in

developing some types of shear reinforcement. The test results of Scavuzzo suggest that failure can occur before the shear reinforcement is sufficiently strained to participate in carrying load. Additives, such as fiber reinforcement, which affect the tensile strength of the concrete without affecting the compressive strength require a re-calibration of α. Some direct measure of tensile strength should be used instead of $\sqrt{f'_c}$.

6.8.2 Beams

If the truss model is valid for flat plates, then it should also apply to slabs with beams and to beams themselves. Truss models are already being used for beams with shear reinforcement. The confinement failure described in Chapter 3 provides an approach for assessing the strength of beams without shear reinforcement. A unified and consistent treatment of shear in reinforced concrete may be attainable.

6.8.3 Relationship to Bar Development

There are marked similarities between the method used in Chapter 3 to estimate α and various plasticity approaches for the estimation of bar development lengths.[6, 15] It is quite possible that the angle of each individual strut is, in fact, a function of the development length of its attendant reinforcing bar.

Chapter 7

Summary and Conclusions

The following four conclusions are central to this thesis.

1. Many of the assumptions made by existing methods for the analysis of a slab-column connection are not in agreement with the observed behavior. As a result, most of these methods cannot be expected to produce consistently accurate predictions of failure loads. Moreover, they are not general analytical tools. For example, a model calibrated for interior column locations is inadequate for edge and corner column locations.
2. The truss model accounts for all aspects of observed slab-column connection behavior. The model, calibrated for interior column tests, is used successfully to predict the failure loads of a wide variety of edge column tests.
3. The truss model presents a new explanation for punching failure. The punching phenomenon is described as a failure of the slab to contain the out-of-plane component of compressive forces within the concrete. This new failure mode is in agreement with observations of test specimens.
4. Attempts have been made to classify slab-column failures as being dominated by either shear or flexure. This approach masks the true nature of such failures. It is more descriptive to use the categories of local

connection failures and overall slab failures. The ultimate capacity of a slab-column system is defined by the lesser of these two independent capacities.

References

1. Elstner R.C. and Hognestad E., "Shearing Strength of Reinforced Concrete Slabs", Journal of the American Concrete Institute, Detroit, Michigan, July 1956.

2. Gosselin D., "The Behavior of Reinforced Concrete Slab-Column Structures with Drop Panels Subjected to Gravity and Lateral Loading", The Royal Military College, Kingston, Ontario, 1984.

3. Hanson N.W. and Hanson J.M., "Shear and Moment Transfer Between Concrete Slabs and Columns", Journal of the Portland Cement Association Research and Development Laboratories, Skoike, Illinois, January 1968.

4. Hawkins N.M., "Shear Strength of Slabs with Moments Transferred to Columns", American Concrete Institute SP-42, Detroit, Michigan, 1974.

5. Hawkins N.M., Fallsen H.B. and Hinojosa R.C., "Influence of Column Rectagularity on the Behavior of Flat Plate Structures", American Concrete Institute SP-30, Detroit, Michigan, 1971.

6. Jirsa, J.O., Lutz L.A. and Gergely P., "Rationale for Suggested Development, Splice and Standard Hook Provisions for Deformed Bars in Tension", Concrete International: Design and Construction, Vol. 1, No. 7, July 1979. pp. 47 - 61.

7. Kane K.A., "Some Model Tests on the Punching Action of Reinforced Concrete Slabs at Edge Columns", Honours Project, The Queen's University of Belfast, 1978.

8. Lamb J.W., "Moment Transfer and Joint Stiffness in Reinforced Concrete Flat Plate-Column Connections", The Royal Military College, Kingston, Ontario, 1984.

9. Masterson D.M. and Long A.E., "The Punching Strength of Slabs, a Flexural Approach Using Finite Elements", American Concrete Institute SP-42, Detroit, Michigan, 1974.

10. Moe J., "Shearing Strength of Reinforced Concrete Slabs and Footings Under Concentrated Loads", Journal of the Portland Cement Association Research and Development Laboratories, Skoike, Illinois, Bulletin D47, April 1961.

11. Neville A.M., *Properties of Concrete*, second (metric) edition, The Copp Clark Publishing Company, Toronto, Canada, 1973.

12. Regan P.E., "Punching Shear in Reinforced Concrete - A State-of-the-Art Report", Polytechnic of Central London, United Kingdom, 1984.

13. Regan P.E., "Behavior of Reinforced Concrete Flat Slabs", Construcion Industry Research and Information Association, London, England, 1981.

14. Regan P.E., Walker P.R. and Zakaria K.A.A., "Tests of Reinforced Concrete Flat Slabs", CIRIA Project RP 220, Polytechnic of Central London, United Kingdom, 1979.

15. Reynolds G.C., "Bond Strength of Deformed Bars in Tension", Technical Report 548, Cement and Concrete Association, Wexham Springs, Slough, 1982.

16. Scavuzzo L., "Shear Reinforcement at Slab-Column Connections in a Reinforced Concrete Flat Plate Structure", The Royal Military College, Kingston, Ontario, 1978.

17. Shilling R.C. and Vanderbilt M.D., "Behavior of Shear Test Structure", Structural Engineering Report #4, Civil Engineering Department, Colorado State University, Fort Collins, Colorado, 1970.

18. Scordelis A.C., Lin T.Y. and Mays H.R., "Shear Strength of Prestressed Lift Slabs", Journal of the American Concrete Institute, Detroit, Michigan

19. Stamenković A. and Chapman J.C. "Local Strength at Column Heads at Flat Slabs Subjected to a Combined Vertical and Horizontal Loading", Proceedings of the Institution of Civil Engineers, Part 2 Research and Theory, London, June 1974.

20. Van Dusen M.H., "Unbalanced Moment and Shear Transfer at Slab-Column Connections: A Literature Review", M.Eng. thesis, University of Toronto, 1985.

21. Zaghlool E.R.F., "Strength and Behavior of Corner and Edge Column-Slab Connections in Reinforced Concrete Flat Plates", Ph.D Thesis, Department of Civil Engineering, University of Calgary, Calgary, Alberta, 1971.

Appendix I: Detailed Calculations for Interaction Diagram

Stamenković and Chapman test apparatus

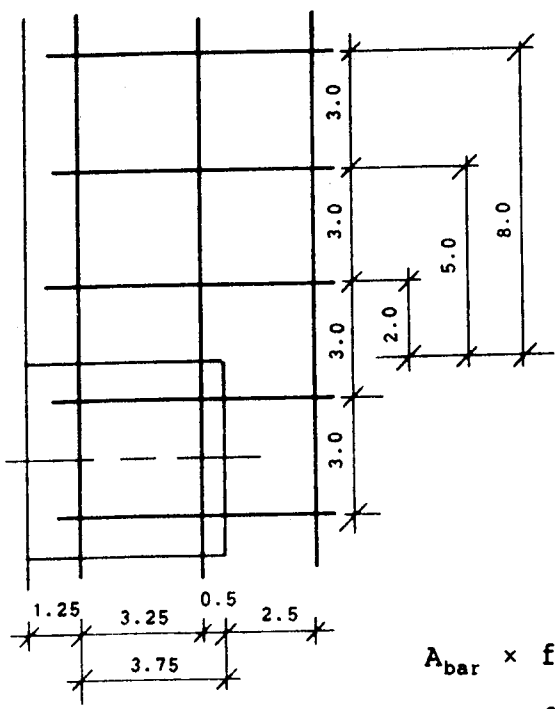

All dimensions in inches. Same mats top and bottom.

$d_s = 2.2 \quad d' = 0.8$

$c_1 = c_2 = 5.0$

$f'_c = 4000$ psi

$f_y = 71.9$ ksi

$A_{bar} = 0.0767$ sq.in.

$A_{bar} \times f_y = 5.52$ kips

$A_{bar} \times f_y \times 0.9d_s = 10.92$ in.kips

Shear Steel:

$$A_{sv}^{T1} = A_{sv}^{B1} = 2 + 2\left(1 - \frac{2.0}{2.2}\right) = 2.18 \text{ bars}$$

$$A_{sv}^{T2} = A_{sv}^{B2} = 4 \text{ bars}$$

Strut Angles:

$$\tan\alpha = 1 - e^{-0.85K} \qquad K = \frac{s_{eff} \times d' \times \sqrt{f'_c}}{A_{bar} \times f_y \times (c/d_s)^{0.25}}$$

Bar A	$s_{eff} = 2.88$	$K = 0.681$	$\tan\alpha = 0.439$
Bar B	$s_{eff} = 3.12$	$K = 0.737$	$\tan\alpha = 0.466$
All others	$s_{eff} = 3.0$	$K = 0.709$	$\tan\alpha = 0.453$

Interaction

1. **Control Point A**

$V_u = 5.52\ (2\times0.439 + 2\times0.466 + 2.18\times0.453) = 15.43$ kips

$M_v = 15.43\times2.5 - 2\times5.52(3.75\times0.439 + 0.5\times0.466)$

$= 17.84$ in.kips

$M_f = 2.18 \times 10.92 = 23.80$ in.kips

2. Flexural steel = 4 bars:

fraction of bar 2 to be anchored $= \frac{2.0}{2.2} = 0.909$

fraction of bar A required for anchoring strut

$= \frac{2.0 \times 0.909}{3.75} = 0.485$

$V_u = 15.43 - 2\times0.485\times5.52\times0.439 = 13.08$ kips

$M_v = 13.08\times2.5 - 2\times5.52(0.515\times3.75\times0.439 + 0.5\times0.466)$

$= 20.78$ in.kips

$M_f = 4 \times 10.92 = 43.68$ in.kips

3. All of bar A used for anchoring strut:

flexural steel $= 4 + 2 \times \frac{3.75-0.485}{5.0} = 4.77$ bars

$V_u = 15.43 - 2\times5.52\times0.439 = 10.59$ kips

$M_v = 10.59\times2.5 - 2\times5.52\times0.5\times0.466 = 23.89$ in.kips

$M_f = 4.77 \times 10.92 = 52.08$ in.kips

4. Check anchoring efficiency of bar B:

$\frac{0.9d_s e_1/e_2}{\tan\alpha_1} = \frac{0.5\times0.9\times2.2}{5.0\times0.466} = 0.425 \quad < \quad 3.25$

Therefore, uplift at A precedes in-plane at B. Bar A^T used for in-plane strut; Bar A^B used for uplift strut.

V_u = 10.59 - 2×5.52×0.439 = 5.74 kips

M_v = 5.74×2.5 + 2×5.52(3.75×0.439 - 0.5×0.466)

= 29.95 in.kips

M_f = 4.77 × 10.92 = 52.08 in.kips

5. Bar B used for anchoring strut:

flexural steel = $4.77 + 2 \times \frac{0.5}{5} = 4.97$ bars

V_u = 5.74 - 2×5.52×0.466 = 0.604 kips

M_v = 0.604×2.5 + 2×5.52×3.75×0.439 = 19.67 in.kips

M_f = 4.97 × 10.92 = 54.27 in.kips

6. **Control Point B**

V_u = 0.604 - 2×5.52×0.466 = -4.54 kips

M_v = -4.54×2.5 + 2×5.52(3.75×0.439 + 0.5×0.466)

= 9.39 in.kips

M_f = 4.97 × 10.92 = 54.27 in.kips

7. **Control Point C**

V_u = -2×5.52(0.439 + 0.466) = -9.98 kips

M_v = -9.98×2.5 + 2×5.52(3.75×0.439 + 0.5×0.466)

= -4.23 in.kips

M_f = 4.97 × 10.92 = 54.27 in.kips

8. **Control Point D**

V_u = V_u at point A' = $-V_u$ at point A = -15.43 kips

M_v = M_v at point A' = $-M_v$ at point A = -17.84 in.kips

M_f = 0.0

Appendix II: Reinforcement Details

The following pages describe reinforcing details for each edge slab-column connection used in this study. Source materials include original project records and theses as well as reports in technical journals. Not all of these documents are complete in their description of the specimens. In those cases where dimensions could not be verified by the experimenter, photographic records of crack patterns and reinforcement prior to casting were used to estimate bar positions. What follows represents a compilation of the best available information regarding the description of each specimen.

Stamenković and Chapman

Six specimens detailed here. Same mats top and bottom. All dimensions in inches.

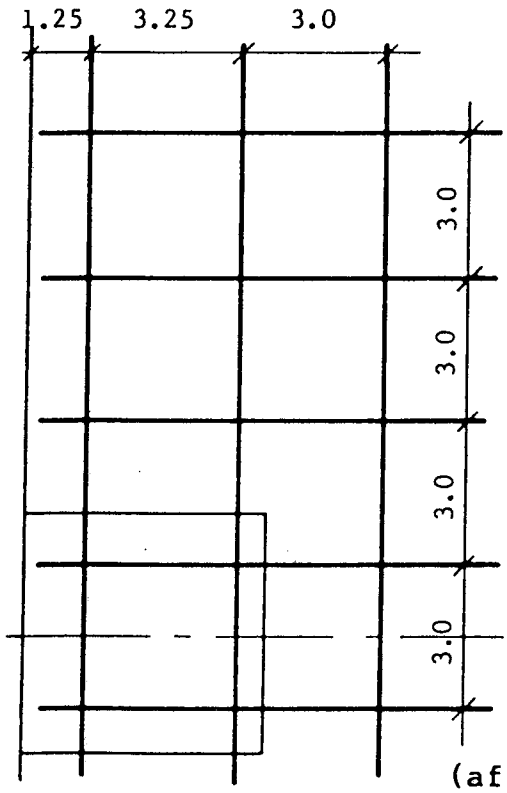

d_s = 2.2
d' = 0.8
t = 3.0
$c_1 = c_2$ = 5.0
d_{bar} = 5/16
A_{bar} = 0.0767 sq.in.

Material properties given below.

(after Stamenković and Chapman)

Mark	f_{cu150} (psi)	f'_c (psi)	f_y (ksi)
V/E/1	5200	4225	71.9
C/E/1	5580	4570	65.0
C/E/2	4700	3780	71.9
C/E/3	4930	3980	71.9
C/E/4	4980	4030	71.9
M/E/2	4800	3870	71.9

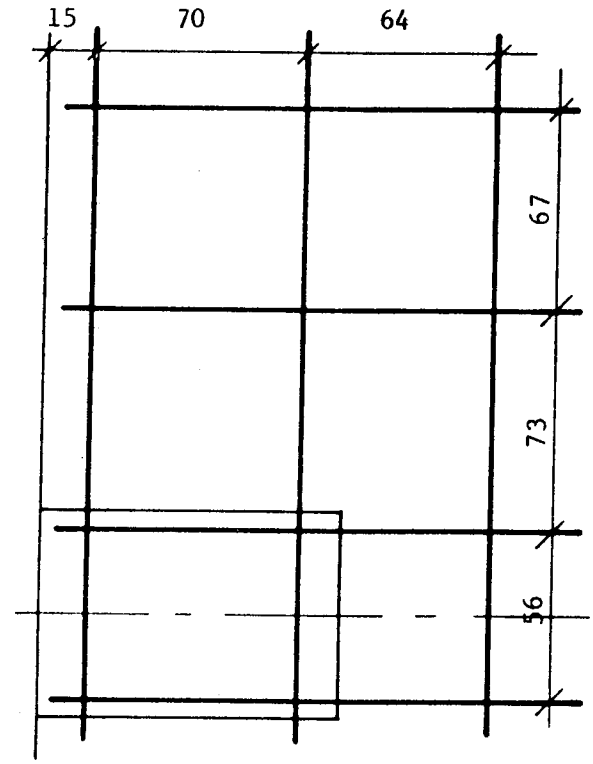

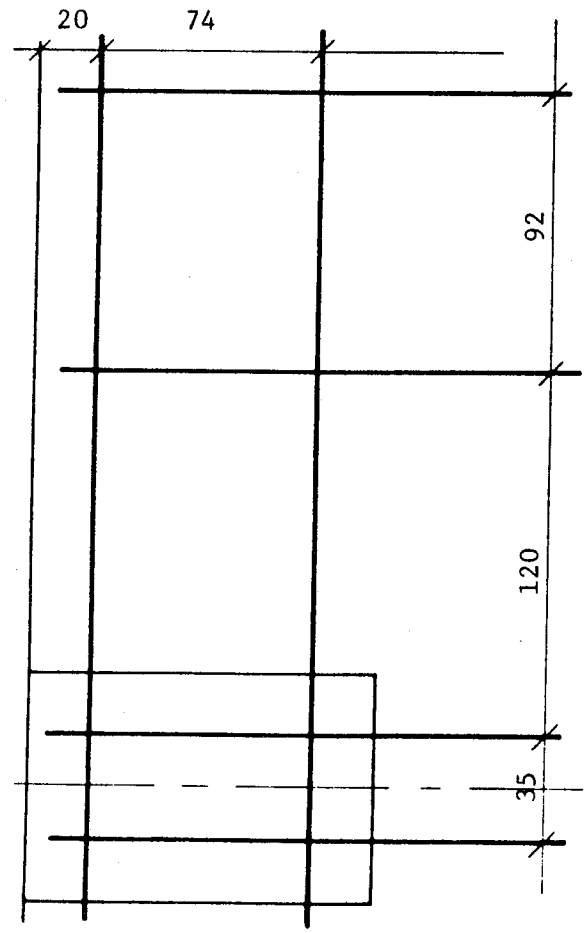

Kane

A total of four specimens are detailed here. Same mats top and bottom. All dimensions are in mm. Same size of flexural reinforcement used in all specimens:

d_{bar} = 6

A_{bar} = 28.3 sq.mm

f_y = 480 MPa

K-1:

t = 51

d_s = 41 d' = 10

c_1 = 100 c_2 = 68

f_{cu150} = 38.5 MPa

f'_c ≅ 30.2 MPa

K-2:

t = 48

d_s = 38 d' = 10

c_1 = 114 c_2 = 75

f_{cu150} = 45.0 MPa

f'_c ≅ 35.9 MPa

(after Kane)

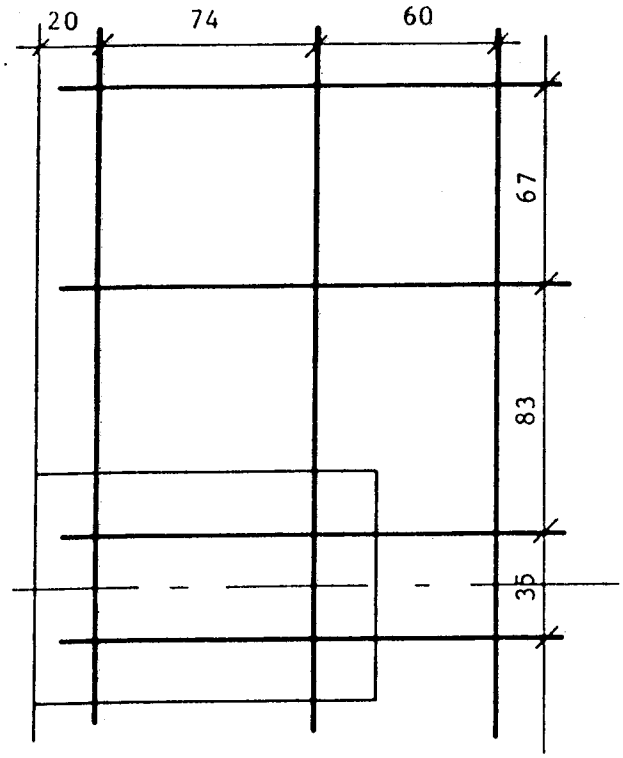

K-3

$t = 48$

$d_s = 38 \quad d' = 10$

$c_1 = 114$

$c_2 = 75$

$f_{cu150} = 51.0$ MPa

$f'_c \cong 41.2$ MPa

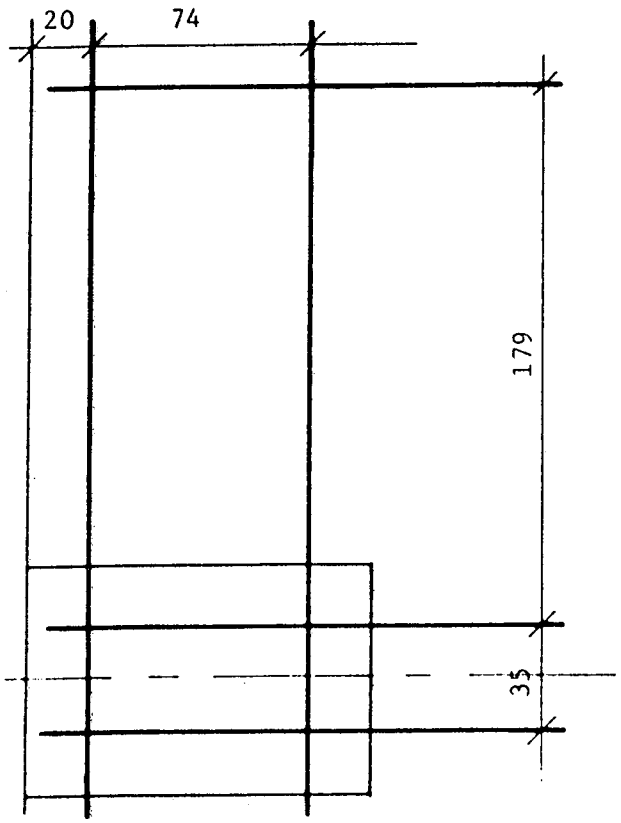

K-4

$t = 48$

$d_s = 38 \quad d' = 10$

$c_1 = 114 \quad c_2 = 75$

$f_{cu150} = 35.3$ MPa

$f'_c \cong 27.6$ MPa

(after Kane)

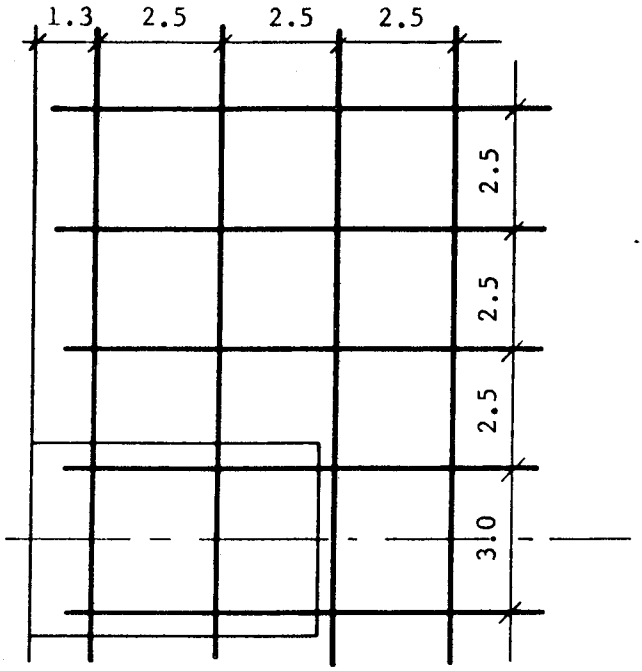

Scavuzzo: S-1

Same mats top and bottom. All dimensions in inches.

$t = 2.5$
$d_s = 1.95$ $d' = 0.55$
$c_1 = 6.0$ $c_2 = 4.0$
$d_{bar} = 0.226$
$A_{bar} = 0.04$ sq.in.
$f_y = 55$ ksi
$f'_c = 5530$ psi

(after Scavuzzo)

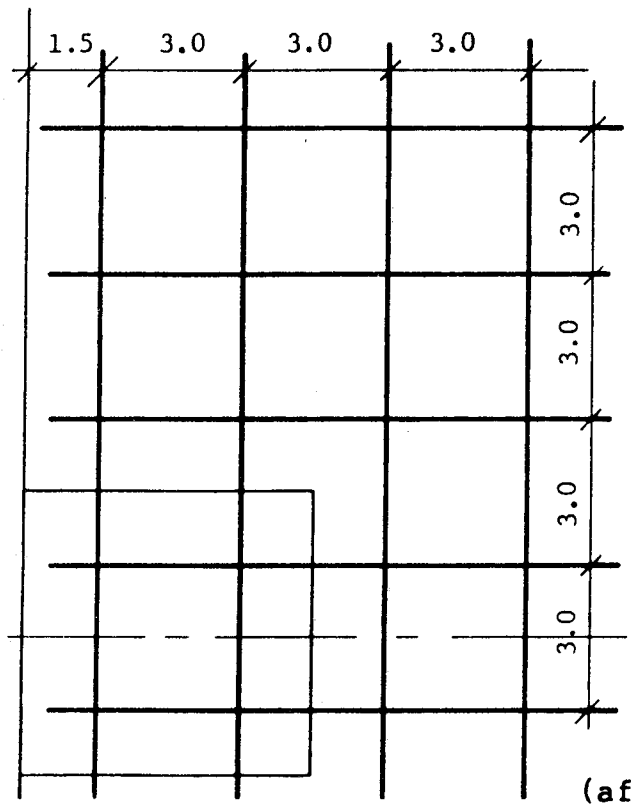

Hanson and Hanson: D15

Same mats top and bottom. All dimensions in inches

$t = 3.0$
$d_s = 2.25$ $d' = 0.75$
$c_1 = c_2 = 6.0$
$d_{bar} = 0.375$ (#3 bar)
$A_{bar} = 0.11$ sq.in.
$f_y = 53$ ksi
$f'_c = 4510$ psi

(after Hanson and Hanson)

Regan

A total of ten double column tests by Regan are detailed here. All dimensions are in mm. For each specimen, the left hand sketch shows the top mat reinforcement while the right hand sketch shows the bottom reinforcement. The following dimensions are common to all specimens except SE2:

t = 125mm d_s = 98mm d' = 27mm

For specimen SE2:

t = 125mm d_s = 101mm d' = 24mm

Three different sizes of bar were used as flexural reinforcement in the slabs. They are:

Type	d_{bar} (mm)	A_{bar} (sq.mm)	f_y (MPa)
D8	8	50.3	480
D10	10	78.5	500
D12	12	113.1	480

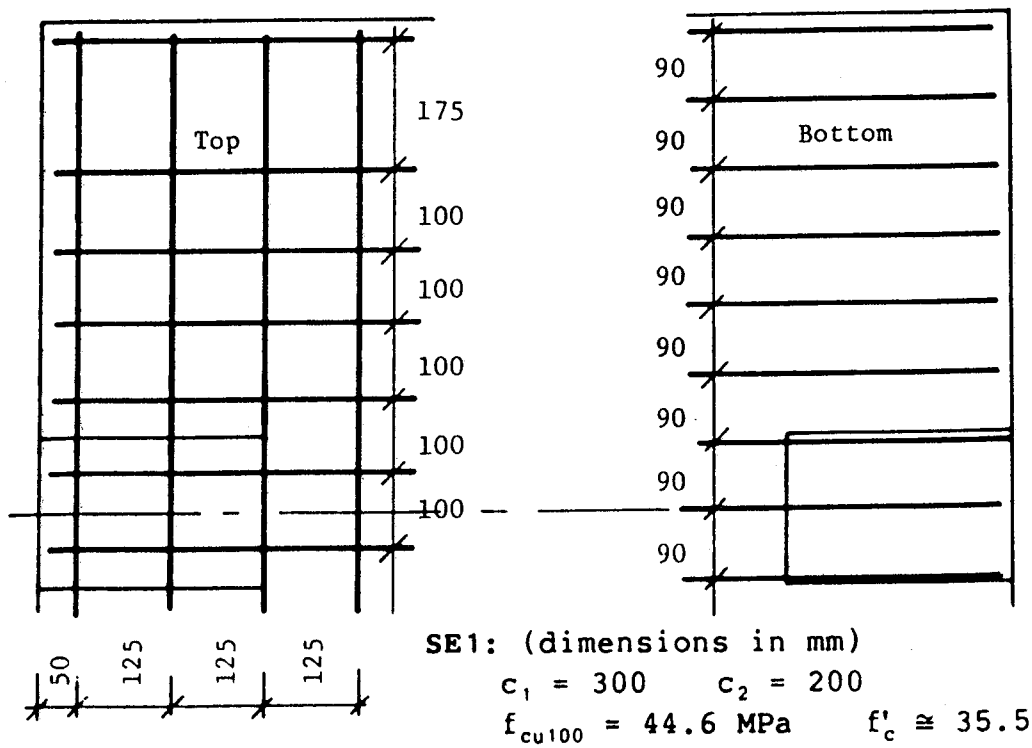

(after Regan)

SE1: (dimensions in mm)

c_1 = 300 c_2 = 200

f_{cu100} = 44.6 MPa $f'_c \cong$ 35.5 MPa

All bars type D12.

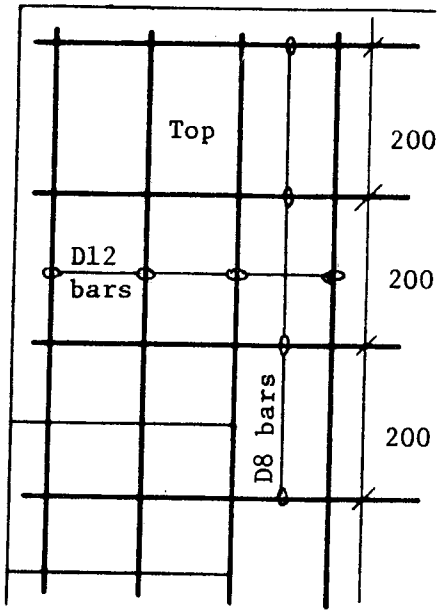

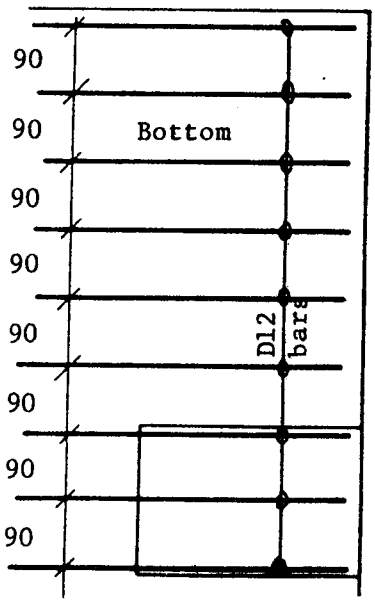

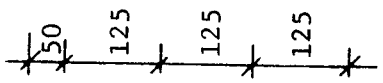

SE2: (dimensions in mm)

c_1 = 300 c_2 = 200

f_{cu100} = 54.6 MPa $f'_c \cong$ 44.4 MPa

(after Regan)

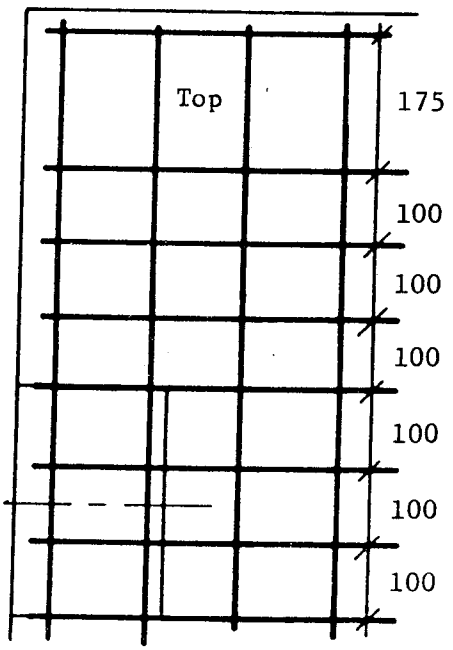

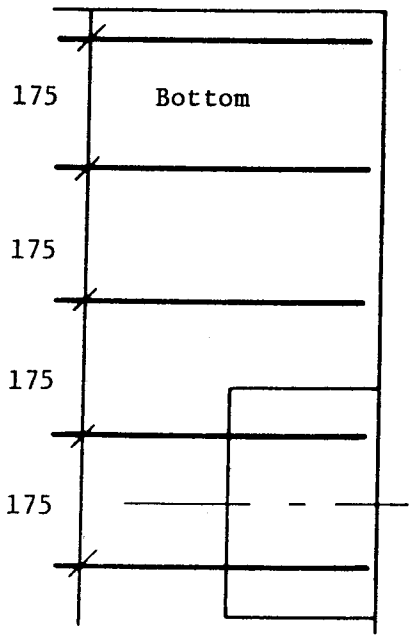

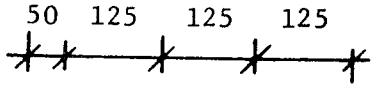

SE4: (dimensions in mm)

c_1 = 200 c_2 = 300

f_{cu100} = 34.3 MPa $f'_c \cong$ 26.6 MPa

All bars type D12.

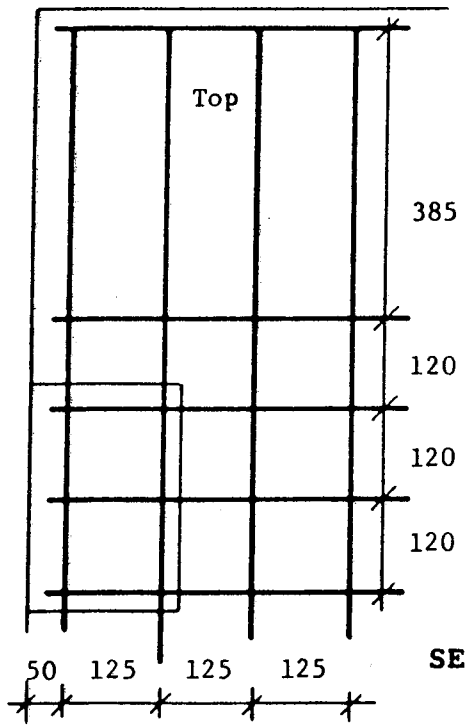

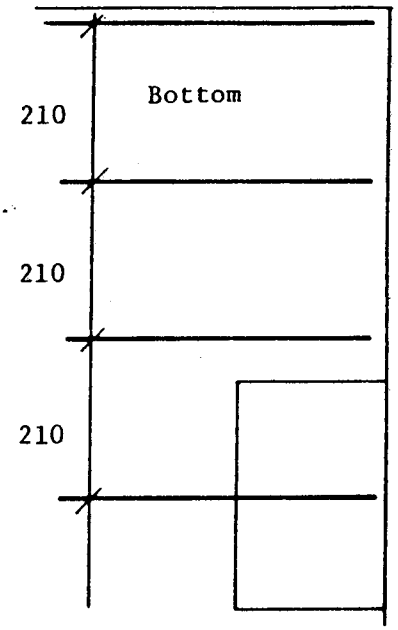

(after Regan)

SE5: (dimensions in mm)

c_1 = 200 c_2 = 300

f_{cu100} = 55.2 MPa $f'_c \cong$ 44.9 MPa

All bars type D12.

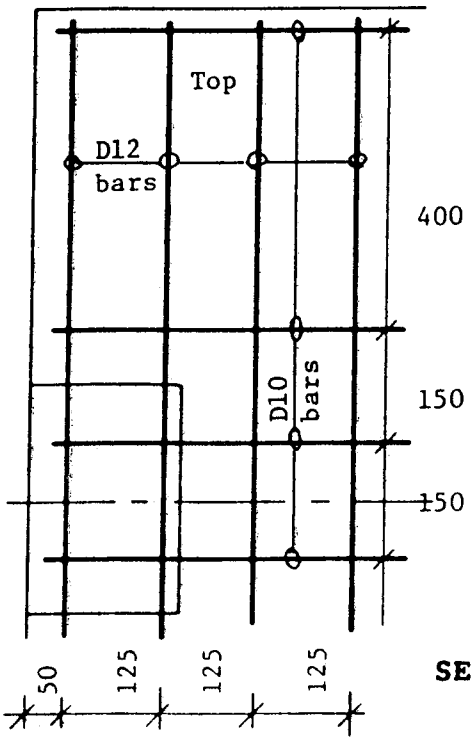

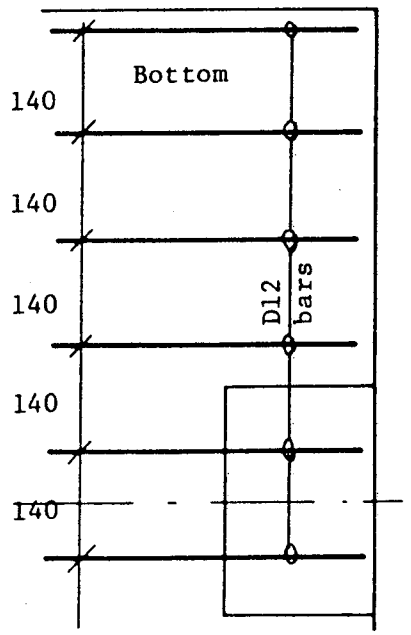

SE6: (dimensions in mm)

c_1 = 200 c_2 = 300

f_{cu100} = 40.0 MPa $f'_c \cong$ 32.9 MPa

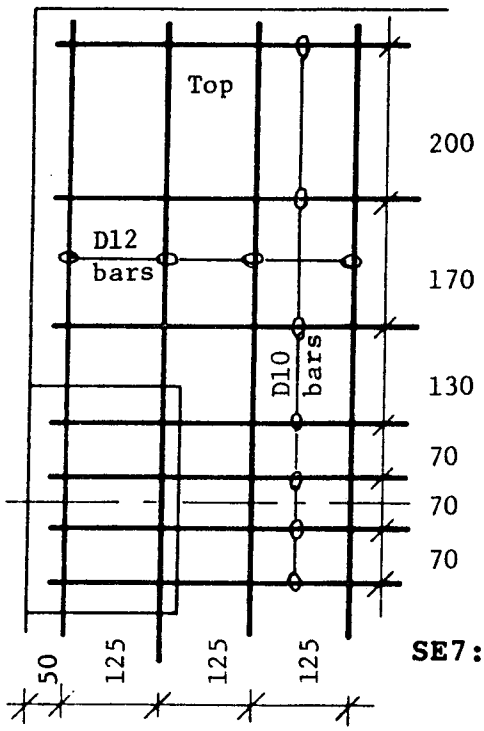

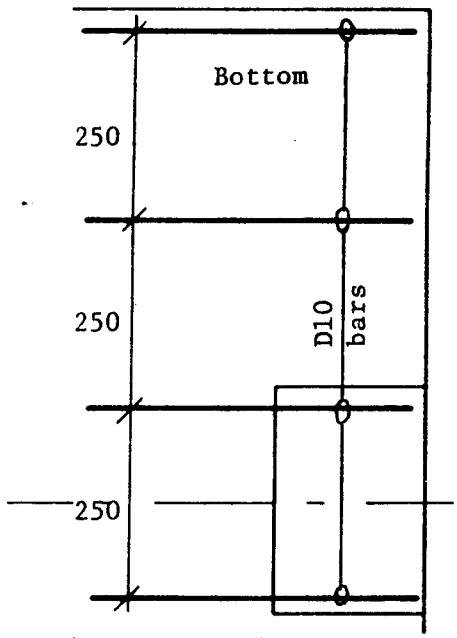

SE7: (dimensions in mm)

c_1 = 200 c_2 = 300

f_{cu100} = 49.5 MPa $f'_c \cong$ 39.8 MPa

(after Regan)

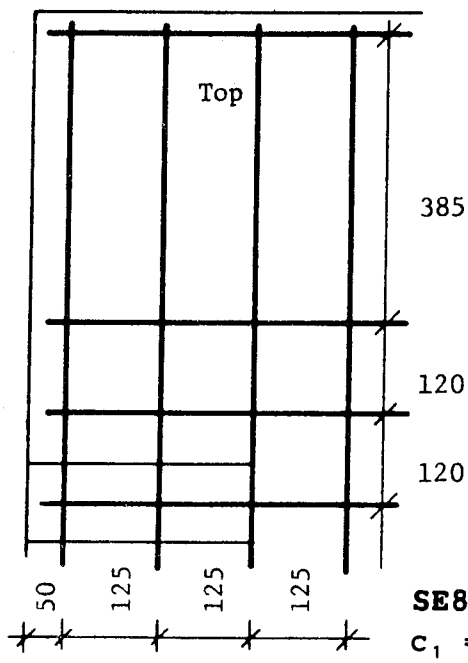

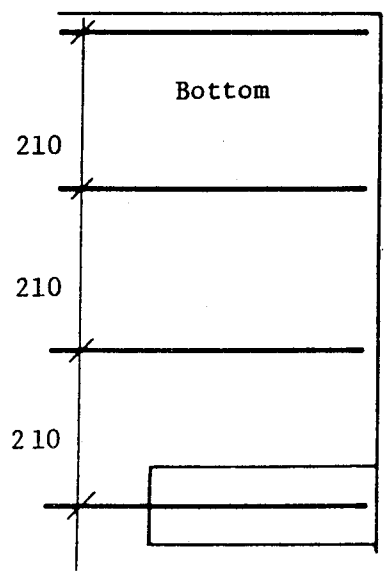

SE8: (dimensions in mm)

c_1 = 300 c_2 = 100

f_{cu100} = 52.0 MPa $f'_c \cong$ 42.1 MPa

All bars type D12.

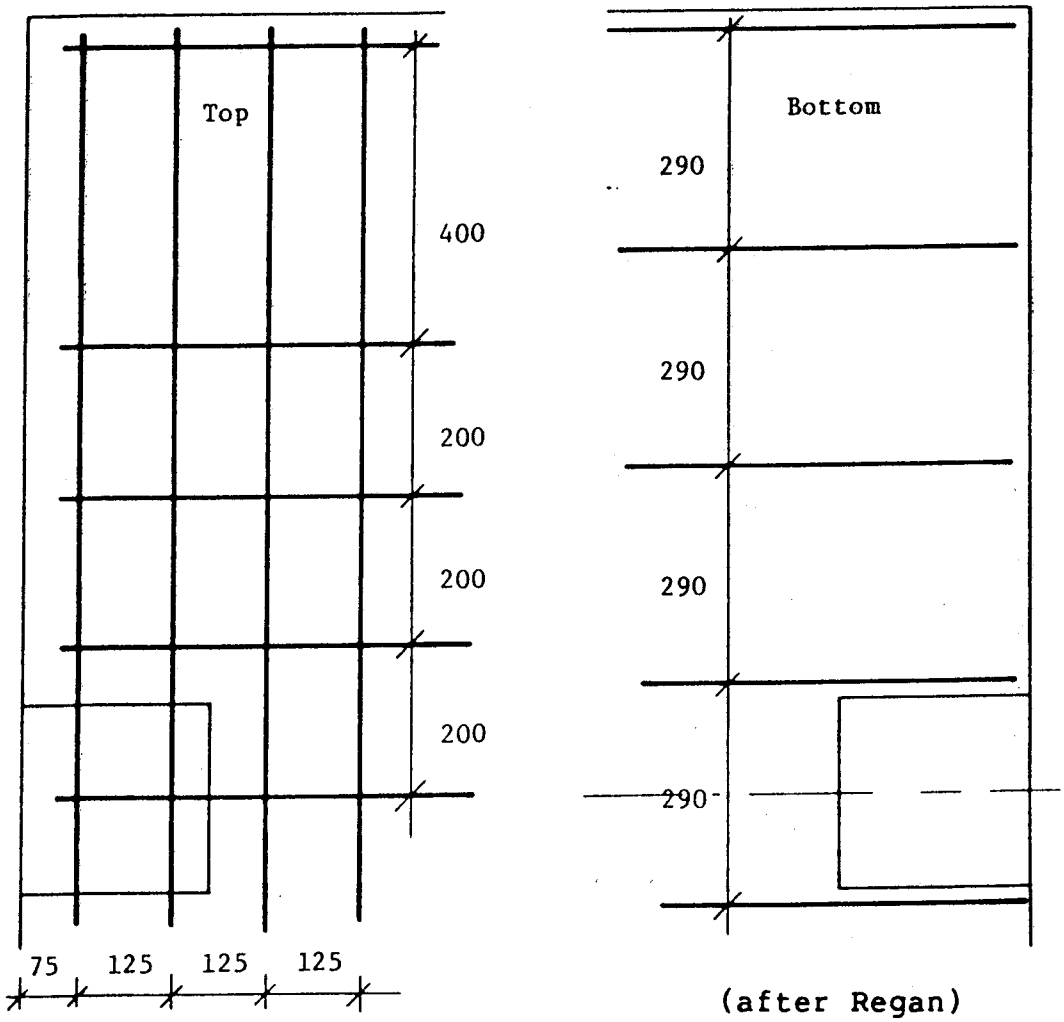

(after Regan)

SE9, SE10 and SE11: (dimensions in mm)

$c_1 = c_2 = 250$ All reinforcement type D12.
Material properties listed below.

Mark	f_{cu100} (MPa)	f'_c (MPa)
SE9	51.8	41.9
SE10	50.9	41.1
SE11	62.5	51.5

Zaghlool

A total of eight specimens are detailed here. All have same mats top and bottom. All dimensions in inches.

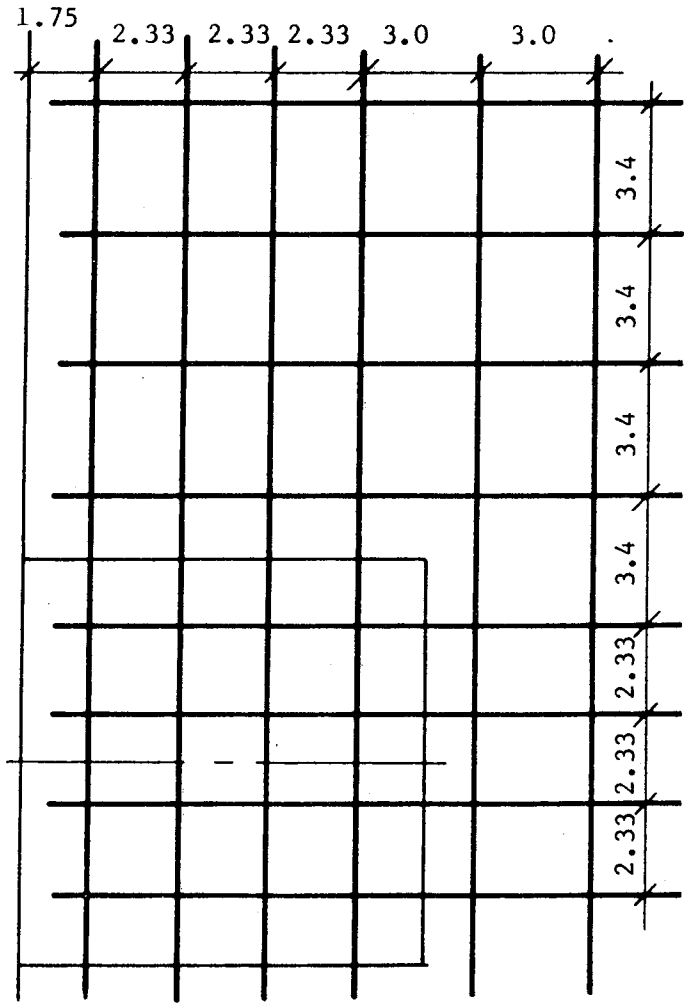

Z-V(1), Z-V(4), Z-V(5) and Z-V(6):

$t = 6$
$d_s = 4.75$
$d' = 1.25$
$c_1 = c_2 = 10.5$
$d_{bar} = 0.5$
(#4 bar)
$A_{bar} = 0.2$ sq.in.

Material properties listed below.

(after Zaghlool)

Mark	f'_c (psi)	f_y (ksi)
Z-V(1)	4980	68.7
Z-V(4)	5080	63.4
Z-V(5)	5100	69.0
Z-V(6)	4540	69.1

Z-V(2): (dimensions in inches)

$t = 6$ $d_s = 4.75$ $d' = 1.25$
$c_1 = c_2 = 10.5$

$d_{bar} = 0.5$ (#4 bar) $A_{bar} = 0.2$ sq.in.

$f_y = 68.7$ ksi $f'_c = 5870$ psi

(after Zaghlool)

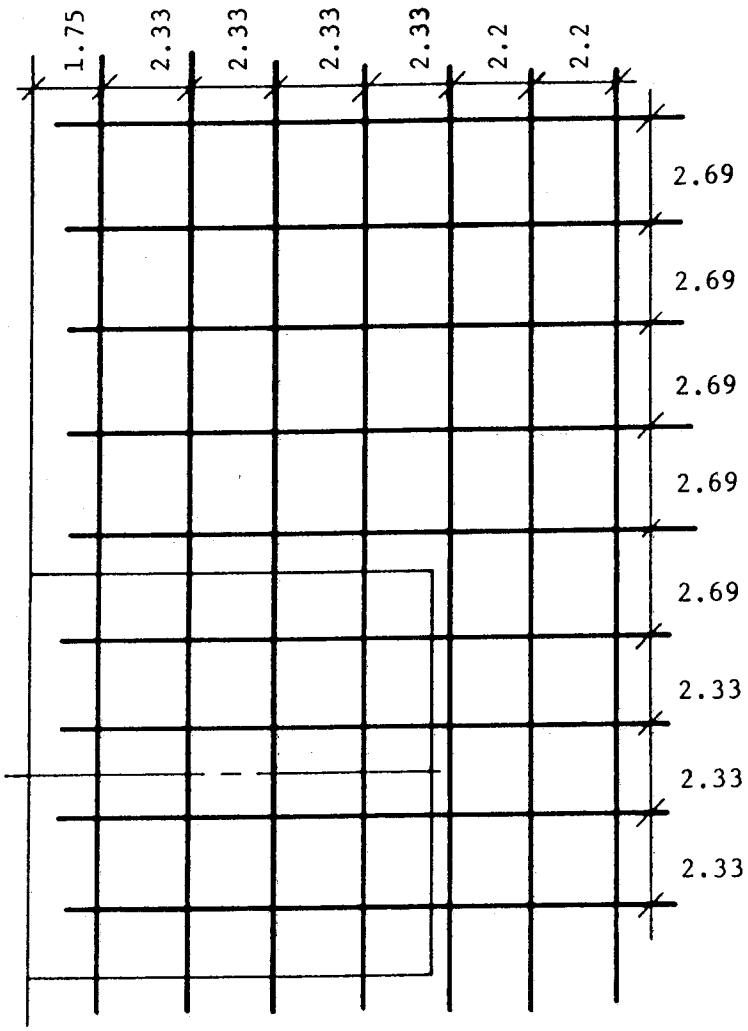

Z-V(3): (dimensions in inches)

$t = 6$ $\quad d_s = 4.625$ $\quad d' = 1.375$
$c_1 = c_2 = 10.5$

Bars passing through column:
$d_{bar} = 0.5$ (#4 bar) $\quad A_{bar} = 0.2$ sq.in.

Remaining bars in slab:
$d_{bar} = 0.625$ (#5 bar) $\quad A_{bar} = 0.31$ sq.in.

$f_y = 68.9$ ksi $\quad f'_c = 5620$ psi

(after Zaghlool)

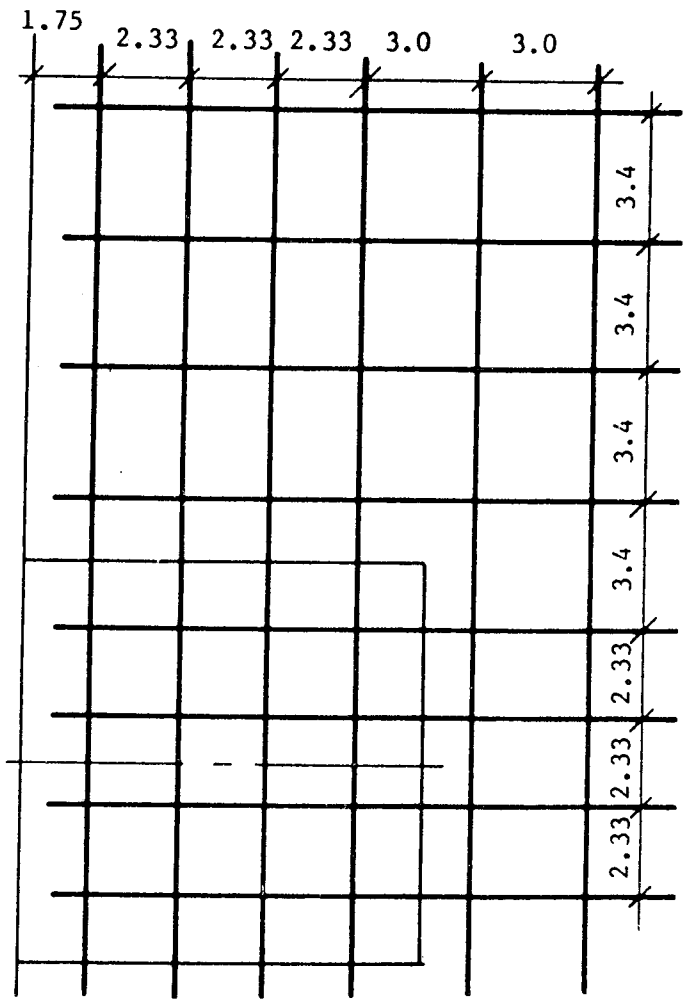

Z-IV(1): (dimensions in inches)

$t = 6$ $d_s = 4.75$ $d' = 1.25$
$c_1 = c_2 = 7.0$

$d_{bar} = 0.5$ (#4 bar) $A_{bar} = 0.2$ sq.in.

$f_y = 69.0$ ksi $f'_c = 3965$ psi

(after Zaghlool)

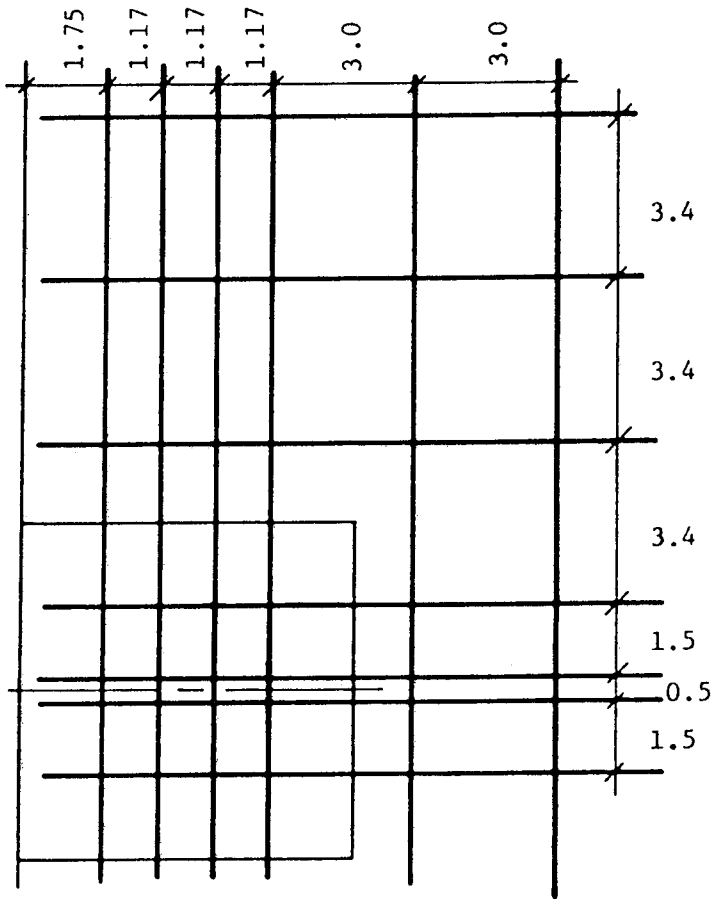

Z-VI(1): (dimensions in inches)

$t = 6$ $d_s = 4.75$ $d' = 1.25$
$c_1 = c_2 = 14.0$

$d_{bar} = 0.5$ (#4 bar) $A_{bar} = 0.2$ sq.in.

$f_y = 69.0$ ksi $f'_c = 3770$ psi

(after Zaghlool)

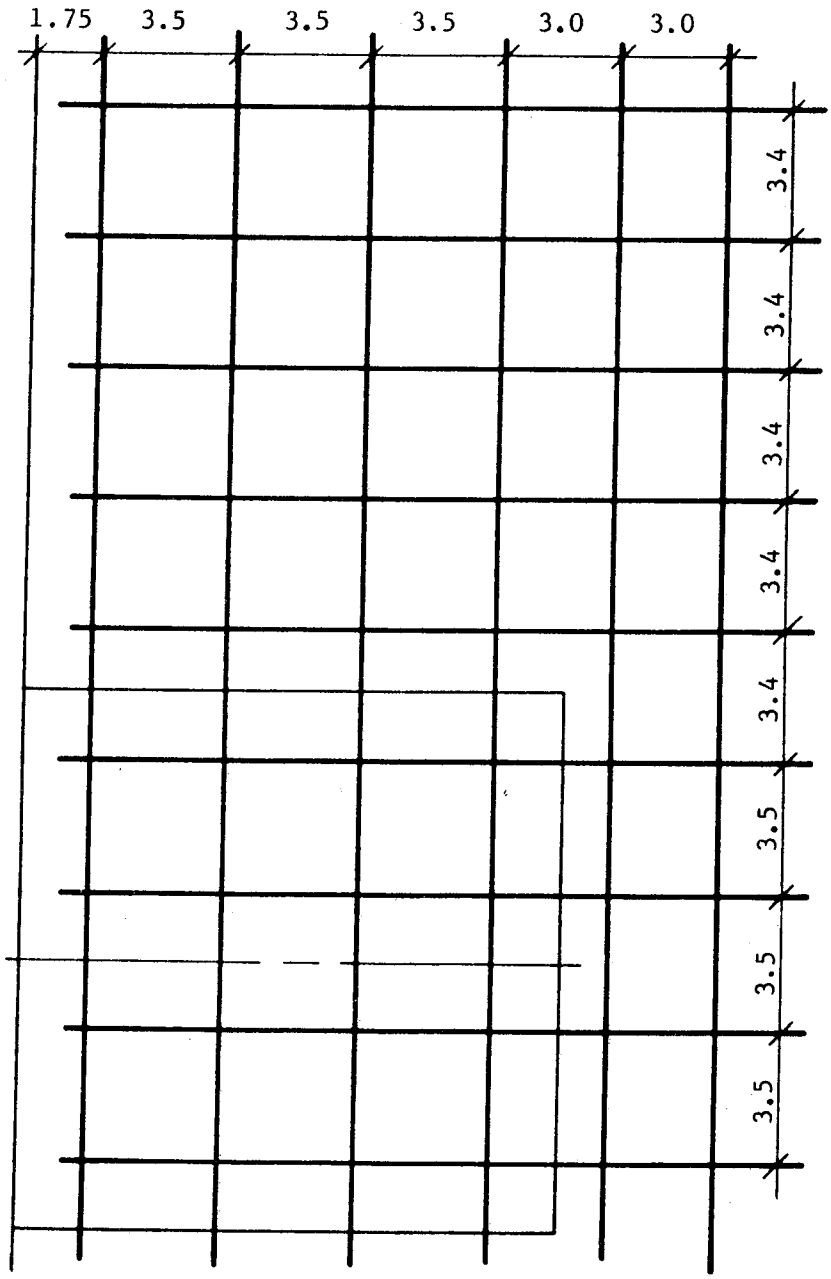

Gosselin

Two specimens are detailed here. Each had the same bottom mat (shown only once). All dimensions are in mm. Same size of flexural reinforcement used in all specimens:

d_{bar} = 5.8
A_{bar} = 25.8 sq.mm
f_y = 375 MPa

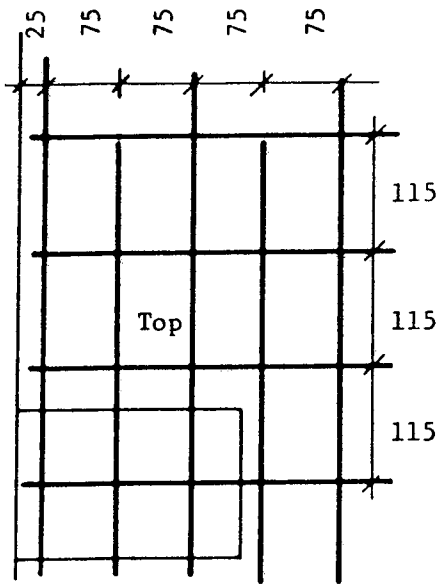

(after Gosselin)

G-1:

t = 79
d_s = 65 d' = 14
c_1 = 225 c_2 = 150
f'_c = 38.1 MPa

G-2:

t = 95
d_s = 81 d' = 14
c_1 = 225 c_2 = 150
f'_c = 39.0 MPa

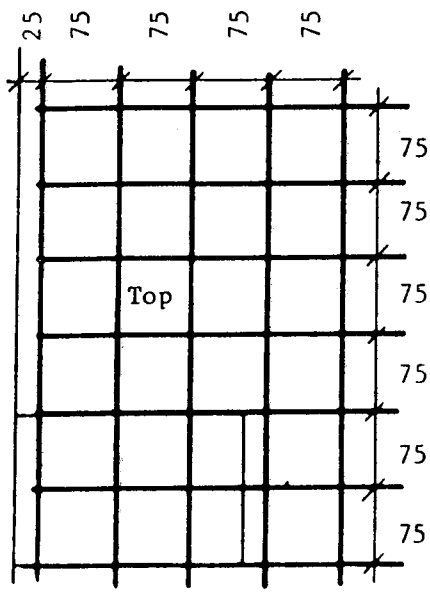

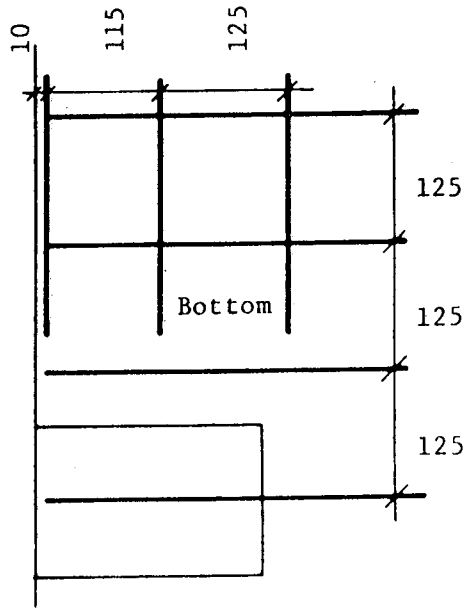

Lamb

Two geometrically similar specimens are detailed here. All dimensions in mm.

$t = 63$ $d_s = 49$ $d' = 14$
$c_1 = 225$ $c_2 = 150$
$d_{bar} = 5.8$ $A_{bar} = 25.8$ sq.mm $f_y = 395$ MPa

L-1: $f'_c = 34.7$ MPa
L-2: $f'_c = 43.8$ MPa

(after Lamb)

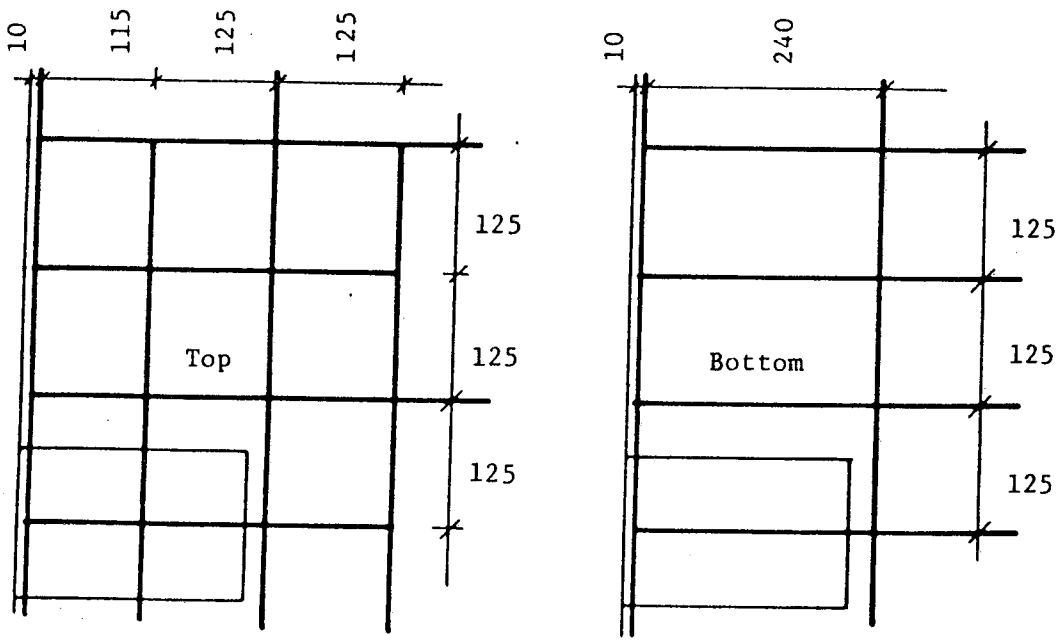

STRUCTURAL ENGINEERING REPORTS

Department of Civil Engineering

University of Alberta

1. *The Behavior of Shear Plates in Sloping Grain Surfaces - No. 1* by J. Longworth, September 1963.

2. *Tests of Eccentrically Loaded Concrete Columns Bent in Double Curvature* by S.L. Barter, May 1964.

3. *The Behavior of Shear Plates in Sloping Grain Surfaces - No. 2* by J. Longworth, June 1964.

4. *Method of Analysis of Shallow Translational Shells* by I. Rajendram and S.H. Simmonds, February 1965.

5. *Torsional Strength and Behavior of Concrete Beams in Combined Loading* by G.S. Pandit and J. Warwaruk, July 1965.

6. *Ultimate Strength and Behavior of Plates* by A. Gyi and S.H. Simmonds, November 1965.

7. *The Behavior of Restrained Reinforced Concrete Columns Under Sustained Load* by R.F. Manuel and J.G. MacGregor, January 1966.

8. *Pretensioned Beams with Confined Compressed Concrete* by R.L. Ward and J. Warwaruk, April 1966.

9. *An Analytical Study of Inclined Cracking in Reinforced Concrete Beams* by J.R.V. Walters and J.G. MacGregor, July 1966.

10. *Rotation Capacity of Wide-Flange Beams under Moment Gradient* by A.F. Lukey and P.F. Adams, May 1967.

11. *Torsional Strength of Rectangular Reinforced Concrete Beams Subjected to Combined Loading* by A.E. McMullen and J. Warwaruk, July 1967.

12. *The Influence of Column Shape on the Behavior of Flat Plate Slabs* by R.J. Kavanagh and S.H. Simmonds, November 1967.

13. *Experiments on Wide-Flange Beams Under Moment Gradient* by R.J. Smith and P.F. Adams, May 1968.

14. *Approximate Analysis of Frame-Shear Wall Structures* by S.N. Guhamajumdar, R.P. Nikhed, J.G. MacGregor and P.F. Adams, May 1968.

15. *Elastic Torsional Analysis of Multi-Story Structures* by J.H. Wynhoven and P.F. Adams, October 1968.

16. *Analysis of Reinforced Concrete Shear Wall-Frame Structures* by W.J. Clark and J.G. MacGregor, November 1968.

17. *Moment Curvature Relations of Prestress Concrete Beams with Confined Compressed Concrete* by M.K. Wilkinson and J. Warwaruk, January 1969.

18. *Fatigue Strength of Deformed Reinforcing Bars* by I.C. Jhamb and J.G. MacGregor, May 1969.

19. *Shallow Shells Supported by Elastic Edge Beams* by D.H. Quapp and S.H. Simmonds, May 1969.

20. *Composite Beams in Negative Bending* by J.H. Davison and J. Longworth, May 1969.

21. *Test of Flat Plate Supported on Columns Elongated in Plan* by A.E. Smith and S.H. Simmonds, May 1969.

22. *Continuous Prestressed Concrete Beams with Confinement* by I.H.G. Duncan and J. Warwaruk, September 1969.

23. *Reinforced Concrete Cellular Orthotropic Slabs* by R.G. Quinton and S.H. Simmonds, October 1969.

24. *Prestressed Concrete Beams with Web Reinforcement Under Combined Loading* by P. Mukherjee and J. Warwaruk, May 1970.

25. *Studies of Reinforced Concrete Shear Wall-Frame Structures* by R.P. Nikhed, J.G. MacGregor and P.F. Adams, June 1970.

26. *Buckling Strengths of Hot Rolled Hot Shaped Sections* by D.A. Heaton and P.F. Adams, July 1970.

27. *Experimental and Analytical Investigation of the Behavior of Coupled Shear Wall-Frame Structures* by S.N.G. Majumdar and P.F. Adams, August 1970.

28. *Comparative Study of Slab-Beam Systems* by J. Misic and S.H. Simmonds, September 1970.

29. *Elastic-Plastic Analysis of Three Dimensional Structures* by J.H. Wynhoven and P.F. Adams, September 1970.

30. *Flexural and Lateral-Torsional Buckling Strengths and Double Angle Struts* by N.J. Nuttall and P.F. Adams, September 1970.

31. *Stiffness Influence Coefficients for Non-Axisymmetric Loading on Closed Cylindrical Shells* by S.H. Iyer and S.H. Simmonds, October 1970.

32. *CSA-S16-1969 Steel Structures for Buildings - Seminar Notes* by P.F. Adams, G.L. Kulak and J. Longworth, November 1970.

33. *Experiments on Steel Wide-Flange Beam-Columns Subjected to Lateral Loads* by G.W. English and P.F. Adams, May 1971.

34. *Finite Element Analysis of Thin-Walled Members of Open Section* by S. Rajasekaran, September 1971.

35. *Finite Element Programs for Beam Analysis* by S. Rajasekaran, September 1971.

36. *Seminar on Building Code Requirements, ACI 318-71* by J.G. MacGregor, S.H. Simmonds and J. Warwaruk, July 1971.

37. *Stability of Braced Frames* by J.H. Davison and P.F. Adams, October 1971.

38. *Time Dependent Deflections of Reinforced Concrete Slabs* by A. Scanlon and D.W. Murray, December 1971.

39. *Fatigue of Reinforcing Bars* by I.C. Jhamb and J.G. MacGregor, February 1972.

40. *Behavior of Welded Connections Under Combined Shear and Moment* by J.L. Dawe and G.L. Kulak, June 1972.

41. *Plastic Design of Steel Frame - Shear Wall Structures* by J. Bryson and P.F. Adams, August 1972.

42. *Solution Techniques for Geometrically Non-linear Structures* by S. Rajasekaran and D.W. Murray, March 1973.

43. *Web Slenderness Limits for Compact Beams* by N.M. Holtz and G.L. Kulak, March 1973.

44. *Inelastic Analysis of Multistory Multibay Frames Subjected to Dynamic Disturbances* by M. Suko and P.F. Adams, June 1973.

45. *Ultimate Strength of Continuous Composite Beams* by S. Hamada and J. Longworth, August 1973.

46. *Prestressed Concrete I-Beams Subjected to Combined Loadings* by D.L.N. Rao and J. Warwaruk, November 1973.

47. *Finite Element Analysis for Combined Loadings with Improved Hexahedrons* by D.L.N. Rao and J. Warwaruk, November 1973.

48. *Solid and Hollow Rectangular Prestressed Concrete Beams Under Combined Loading* by J. Misic and J. Warwaruk, September 1974.

49. *The Second-Order Analysis of Reinforced Concrete Frames* by S.E. Hage and J.G. MacGregor, October 1974.

50. *Web Slenderness Limits for Compact Beam-Columns* by M.J. Perlynn and G.L. Kulak, September 1974.

51. *Web Slenderness Limits for Non-Compact Beams* by N.M. Holtz and G.L. Kulak, August 1975.

52. *Decision Table Processing of the Canadian Standards Association Specification S16.1* by S.K.F. Wu and D.W. Murray, February 1976.

53. *Web Slenderness Limits for Non-Compact Beam-Columns* by D.S. Nash and G.L. Kulak, March 1976.

54. *A Monte Carlo Study of the Strength Variability of Rectangular Tied Reinforced Concrete Columns* by L.H. Grant and J.G. MacGregor, March 1976.

55. *An Elastic Stress Analysis of a Gentilly Type Containment Structure - Volume 1* by D.W. Murray and M. Epstein, April 1976.

56. *An Elastic Stress Analysis of a Gentilly Type Containment Structure - Volume 2 - (Appendices B to F)* by D.W. Murray and M. Epstein, April 1976.

57. *A System of Computer Programs for the Large Deformation In-Plane Anaysis of Beams* by M. Epstein and D.W. Murray, May 1976.

58. *A Statistical Study of Variables Affecting the Strength of Reinforced Normal Weight Concrete Members* by S.A. Mirza and J.G. MacGregor, December 1976.

59. *The Destabilizing Forces Caused by Gravity Loads Acting on Initially Out-of-Plumb Members in Structures* by D. Beaulieu and P.F. Adams, February 1977.

60. *The Second-Order Analysis and Design of Reinforced Concrete Frames* by G.S. Mathews and J.G. MacGregor, January 1977.

61. *The Effects of Joint Eccentricity in Open Web Steel Joists* by R.A. Matiisen, S.H. Simmonds and D.W. Murray, June 1977.

62. *Behavior of Open Web Steel Joists* by R.A. Kaliandasani, S.H. Simmonds and D.W. Murray, July 1977.

63. *A Classical Flexibility Analysis for Gentilly Type Containment Structures* by D.W. Murray, A.M. Rohardt and S.H. Simmonds, June 1977.

64. *Substructure Analysis of Plane Frames* by A.E. Elwi and D.W. Murray, June 1977.

65. *Strength and Behavior of Cold-Formed HSS Columns* by R. Bjorhovde, December 1977.

66. *Some Elementary Mechanics of Explosive and Brittle Failure Modes in Prestressed Containments* by D.W. Murray, June 1978.

67. *Inelastic Analysis of Prestressed Concrete Secondary Containments* by D.W. Murray, L. Chitnuyanondh, C. Wong and K.Y Rijub-Agha, July 1978.,

68. *Strength of Variability of Bonded Prestressed Concrete Beams* by D.K. Kikuchi, S.A. Mirza and J.G. MacGregor, August 1978.

69. *Numerical Analysis of General Shells of Revolution Subjected to Arbitrary Loading* by A.M. Shazly, S.H. Simmonds and D.W. Murray, September 1978.

70. *Concrete Masonry Walls* by M. Hatzinikolas, J. Longworth and J. Warwaruk, September 1978.

71. *Experimental Data for Concrete Masonry Walls* by M. Hatzinikolas, J. Longworth and J. Warwaruk, September 1978.

72. *Fatigue Behavior of Steel Beams with Welded Details* by G.R. Bardell and G.L. Kulak, September 1978.

73. *Double Angle Beam-Column Connections* by R.M. Lasby and R. Bjorhovde, April 1979.

74. *An Effective Uniaxial Tensile Stress-Strain Relationship for Prestressed Concrete* by L. Chitnuyannondh, S. Rizkalla, D.W. Murray and J.G. MacGregor, February 1979.

75. *Interaction Diagrams for Reinforced Masonry* by C. Feeg and J. Warwaruk, April 1979.

76. *Effects of Reinforcement Detailing for Concrete Masonry Columns* by C. Feeg, J. Longworth and J. Warwaruk, May 1979.

77. *Interaction of Concrete Masonry Bearing Walls and Concrete Floor Slabs* by N. Ferguson, J. Longworth and J. Warwaruk, May 1979.

78. *Analysis of Prestressed Concrete Wall Segments* by B.D.P. Koziak and D.W. Murray, June 1979.

79. *Fatigue Strength of Welded Steel Elements* by B.D.P. Koziak and D.W. Murray, June 1979.

80. *Leakage Tests of Wall Segments of Reactor Containments* by S.K. Rizkalla, S.H. Simmonds and J.G. MacGregor, October 1979.

81. *Tests of Wall Segments from Reactor Containments* by S.H. Simmonds, S.H. Rizkalla and J.G. MacGregor, October 1979.

82. *Cracking of Reinforced and Prestressed Concrete Wall Segmenets* by J.G. MacGregor, S.H. Rizkalla and S.H. Simmonds, October 1979.

83. *Inelastic Behavior of Multistory Steel Frames* by M. El Zanaty, D.W. Murray and R. Bjorhovde, April 1980.

84. *Finite Element Programs for Frame Analysis* by M. El Zanaty and D.W. Murray, April 1980.

85. *Test of a Prestressed Concrete Secondary Containment Structure* by J.G. MacGregor, S.H. Simmonds, and S.H. Rizkalla, April 1980.

86. *An Inelastic Analysis of the Gentilly-2 Secondary Containment Structure* by D.W. Murray, C. Wong, S.H. Simmonds and J.G. MacGregor, April 1980.

87. *Nonlinear Analysis of Axisymmetric Reinforced Concrete Structures* by A.E. Elwi and D.W. Murray, May 1980.

88. *Behavior of Prestressed Concrete Containment Structures - A Summary of Findings* by J.G. MacGregor, D.W. Murray, S.H. Simmonds, April 1980.

89. *Deflection of Composite Beams at Service Load* by L. Samantaraya and J. Longworth, June 1980.

90. *Analysis and Design of Stub-Girders* by T.J.E. Zimmerman and R. Bjorhovde, August 1980.

91. *An Investigation of Reinforced Concrete Block Masonry Columns* by G.R. Sturgeon, J. Longworth and J. Warwaruk, September 1980.

92. *An Investigation of Concrete Masonry Wall and Concrete Slab Interaction* by R.M. Pacholok, J. Warwaruk and J. Longworth, October 1980.

93. *FEPARCS5 - A Finite Element Program for the Analysis of Axisymmetric Reinforced Concrete Structures - Users Manual* by A. Elwi and D.W. Murray, November 1980.

94. *Plastic Design of Reinforced Concrete Slabs* by D.M. Rogowsky and S.H. Simmonds, November 1980.

95. *Local Buckling of W Shapes Used as Columns, Beams, and Beam-Columns* by J.L. Dawe and G.L. Kulak, March 1981.

96. *Dynamic Response of Bridge Piers to Ice Forces* by E.W. Gordon and C.J. Montgomery, May 1981.

97. *Full-Scale Test of a Composite Truss* by R. Bjorhovde, June 1981.

98. *Design Methods for Steel Box-Girder Support Diaphragms* by R.J. Ramsay and R. Bjorhovde, July 1981.

99. *Behavior of Restrained Masonry Beams* by R. Lee, J. Longworth and J. Warwaruk, October 1981.

100. *Stiffened Plate Analysis by the Hybrid Stress Finite Element Method* by M.M. Hrabok and T.M. Hrudey, October 1981.

101. *Hybslab - A Finite Element Program for Stiffened Plate Analysis* by M.M. Hrabok and T.M. Hrudey, November 1981.

102. *Fatigue Strength of Trusses Made From Rectangular Hollow Sections* by R.B. Ogle and G.L. Kulak, November 1981.

103. *Local Buckling of Thin-Walled Tubular Steel Members* by M.J. Stephens, G.L. Kulak and C.J. Montgomery, February 1982.

104. *Test Methods for Evaluating Mechanical Properties of Waferboard: A Preliminary Study* by M. MacIntosh and J. Longworth, May 1982.

105. *Fatigue Strength of Two Steel Details* by K.A. Baker and G.L. Kulak, October 1982.

106. *Designing Floor Systems for Dynamic Response* by C.M. Matthews, C.J. Montgomery and D.W. Murray, October 1982.

107. *Analysis of Steel Plate Shear Walls* by L. Jane Thorburn, G.L. Kulak, and C.J. Montgomery, May 1983.

108. *Analysis of Shells of Revolution* by N. Hernandez and S.H. Simmonds, August 1983.

109. *Tests of Reinforced Concrete Deep Beams* by D.M. Rogowsky, J.G. MacGregor and S.Y. Ong, September 1983.

110. *Shear Strength of Deep Reinforced Concrete Continuous Beams* by D.M. Rogowsky and J.G. MacGregor, September 1983.

111. *Drilled-In Inserts in Masonry Construction* by M.A. Hatzinikolas, R. Lee, J. Longworth and J. Warwaruk, October 1983.

112. *Ultimate Strength of Timber Beam Columns* by T.M. Olatunji and J. Longworth, November 1983.

113. *Lateral Coal Pressures in a Mass Flow Silo* by A.B.B. Smith and S.H. Simmonds, November 1983.

114. *Experimental Study of Steel Plate Shear Walls* by P.A. Timler and G.L. Kulak, November 1983.

115. *End Connection Effects on the Strength of Concrete Filled HSS Columns* by S.J. Kennedy and J.G. MacGregor, April 1984.

116. *Reinforced Concrete Column Design Program* by C-K. Leung and S.H. Simmonds, April 1984.

117. *Deflections of Two-way Slabs under Construction Loading* by C. Graham and A. Scanlon, August 1984.

118. *Effective Lengths of Laterally Unsupported Steel Beams* by C.D. Schmitke and D.J.L. Kennedy, October 1984.

119. *Flexural and Shear Behaviour of Large Diameter Steel Tubes* by R.W. Bailey and G.L. Kulak, November 1984.

120. *Concrete Masonry Prism Response due to Loads Parallel and Perpendicular to Bed Joints* by R. Lee, J. Longworth and J. Warwaruk.

121. *Standardized Flexible End Plate Connections for Steel Beams* by G.J. Kriviak and D.J.L. Kennedy, December 1984.

122. *The Effects of Restrained Shrinkage on Concrete Slabs* by K.S.S. Tam and A. Scanlon, December 1984.

123. *Prestressed Concrete Beams with Large Rectangular Web Openings* by T. do M.J. Alves and A. Scanlon, December 1984.

124. *Tests on Eccentrically Loaded Fillet Welds* by G.L. Kulak and P.A. Timler, December 1984.

125. *Analysis of Field Measured Deflections Scotia Place Office Tower* by A. Scanlon and E. Ho, December 1984.

126. *Ultimate Behaviour of Continuous Deep Reinforced Concrete Beams* by D.R. Ricketts and J.G. MacGregor, January 1985.

127. *The Interaction of Masonry Veneer and Steel Studs in Curtain Wall Construction* by W.M. McGinley, J. Warwaruk, J. Longworth and M. Hatzinikolas, May 1985.

128. *Evaluation of Existing Bridge Structure by Nondestructive Test Methods* by L. Mikhailovsky and A. Scanlon, May 1985.

129. *Finite Element Modelling of Buried Structures* by D.K. Playdon and S.H. Simmonds, October 1985.

130. *Behaviour and Ultimate Strength of Transversely Loaded Continuous Steel Plates* by K.P. Ratzlaff and D.J.L. Kennedy, November 1985.

131. *Inelastic Lateral Buckling of Steel Beam-Columns* by P.E. Cuk, M.A. Bradford and N.S. Trahair, December 1985.

132. *Design Strengths of Steel Beam-Columns* by N.S. Trahair, December 1985.

133. *Behaviour of Fillet Welds as a Function of the Angle of Loading* by G.S. Miazga and D.J.L. Kennedy, March 1986.

134. *Inelastic Seismic Response of Precast Concrete Large Panel Coupled Shear Wall Systems* by M.R. Kianoush and A. Scanlon, March 1986.

135. *Finite Element Prediction of Bin Loads* by A.H. Askari and A.E. Elwi, June 1986.

136. *Shear Behavior of Large Diameter Fabricated Steel Cylinders* by J. Mok and A.E. Elwi, June 1986.

137. *Local Buckling Rules for Structural Steel Members* by S. Bild and G.L. Kulak, May 1986.

138. *Finite Element Prediction of Reinforced Concrete Behavior: Vol. I - Beams* by S. Balakrishnan and D.W. Murray, July 1986.

139. *Finite Element Prediction of Reinforced Concrete Behavior: Vol. II - Panels* by S. Balakrishnan and D.W. Murray, July 1986.

140. *Finite Element Prediction of Reinforced Concrete Behavior: Vol. III - Influence of Modeling* by S. Balakrishnan and D.W. Murray, July 1986.

141. *Shear-Moment Transfer in Slab-Column Connections* by S.D.B. Alexander and S.H. Simmonds, July 1986.